

SOUTHWEST RESEARCH INSTITUTE  
Post Office Drawer 28510, 6220 Culebra Road  
San Antonio, Texas 78284

REACTOR VESSEL MATERIAL  
SURVEILLANCE PROGRAM FOR  
DONALD C. COOK UNIT NO. 1  
ANALYSIS OF CAPSULE T

by  
E. B. Norris

FINAL REPORT  
SwRI Project 02-4770

to  
American Electric Power Service Corporation  
2 Broadway  
New York, New York 10004

December 8, 1977

APPROVED	
IN GENERAL	
ENGINEERING DEPARTMENT AMERICAN ELECTRIC POWER SERVICE CORP.	
PER <u>JR Jensen</u>	DATE <u>5/25/78</u>

Approved:

U. S. Lindholm

U. S. Lindholm, Director  
Department of Materials Sciences

8002270331

## TABLE OF CONTENTS

	<u>Page</u>
LIST OF TABLES	iii
LIST OF FIGURES	v
I. SUMMARY OF RESULTS AND CONCLUSIONS	1
II. BACKGROUND	3
III. DESCRIPTION OF MATERIAL SURVEILLANCE PROGRAM	7
IV. TESTING OF SPECIMENS FROM CAPSULE T	13
V. ANALYSIS OF RESULTS	35
VI. HEATUP AND COOLDOWN LIMIT CURVES FOR NORMAL OPERATION OF DONALD C. COOK UNIT NO. 1	43
VII. REFERENCES	47
APPENDIX A - TENSILE TEST RECORDS	A-1
APPENDIX B - PROCEDURE FOR THE GENERATION OF ALLOWABLE PRESSURE-TEMPERATURE LIMIT CURVES FOR NUCLEAR POWER PLANT REACTOR VESSELS	B-1



# LIST OF TABLES

<u>Table</u>		<u>Page</u>
I	Donald C. Cook Unit No. 1 Reactor Vessel Surveillance Materials	9
II	Summary of Reactor Operations Donald C. Cook Unit No. 1	16
III	Summary of Neutron Dosimetry Results Donald C. Cook Unit No. 1--Capsule T	17
IV	Fast Neutron Spectrum and Iron Activation Cross Sections for Capsule T	19
V	Charpy V-Notch Impact Data The Donald C. Cook Unit No. 1 Reactor Pressure Vessel Intermediate Shell Plate B4406-3 (Longitudinal Direction)	21
VI	Charpy V-Notch Impact Data The Donald C. Cook Unit No. 1 Reactor Pressure Vessel Intermediate Shell Plate B4406-3 (Transverse Direction)	22
VII	Charpy V-Notch Impact Data The Donald C. Cook Unit No. 1 Reactor Pressure Vessel Core Region Weld Metal	23
VIII	Charpy V-Notch Impact Data The Donald C. Cook Unit No. 1 Reactor Pressure Vessel Core Region Weld Heat-Affected Zone Metal	24
IX	Charpy V-Notch Impact Data A533 Grade B Class 1 Correlation Monitor Material	25
X	Notch Toughness Properties of Capsule T Specimens Donald C. Cook Unit No. 1	31
XI	Tensile Properties of Surveillance Materials Capsule T	32
XII	Projected Values of $RT_{NDT}$ for Donald C. Cook Unit No. 1 for Up to 12 EFPY of Operation	40

LIST OF TABLES (CONT'D.)

<u>Table</u>		<u>Page</u>
XIII	Projected Values of $RT_{NDT}$ for Donald C. Cook Unit No. 1 for Up to 32 EFPY of Operation	41
XIV	Proposed Reactor Vessel Surveillance Capsule Schedule Donald C. Cook Unit No. 1	42

# LIST OF FIGURES

<u>Figure</u>		<u>Page</u>
1	Arrangement of Surveillance Capsules in the Pressure Vessel	8
2	Vessel Material Surveillance Specimens	11
3	Arrangement of Specimens and Dosimeters in Capsule T	12
4	Charpy V-Notch Properties of Plate B4406-3 (Long.) Donald C. Cook Unit No. 1 Surveillance Program	26
5	Charpy V-Notch Properties of Plate B4406-3 (Trans.) Donald C. Cook Unit No. 1 Surveillance Program	27
6	Charpy V-Notch Properties of Core Region Weld Metal Donald C. Cook Unit No. 1 Surveillance Program	28
7	Charpy V-Notch Properties of Core Region HAZ Material Donald C. Cook Unit No. 1 Surveillance Program	29
8	Charpy V-Notch Properties of Correlation Monitor Material Donald C. Cook Unit No. 1 Surveillance Program	30
9	Dependence of $C_v$ Shelf Energy on Neutron Fluence, Donald C. Cook Unit No. 1	37
10	Effect of Neutron Fluence on $RT_{NDT}$ Shift, Donald C. Cook Unit No. 1	38
11	Donald C. Cook Unit No. 1 Reactor Coolant Heatup Limitations Applicable for Periods Up to 12 Effective Full Power Years	45
12	Donald C. Cook Unit No. 1 Reactor Coolant Cooldown Limitations Applicable for Periods Up to 12 Effective Full Power Years	46



## I. SUMMARY OF RESULTS AND CONCLUSIONS

The analysis of the first material surveillance capsule removed from the Donald C. Cook Unit No. 1 reactor pressure vessel led to the following conclusions:

(1) Based on a calculated neutron spectral distribution, Capsule T received a fast fluence of  $1.80 \times 10^{18}$  neutrons/cm<sup>2</sup> > 1 MeV.

(2) The surveillance specimens of the core beltline materials experienced shifts in transition temperature of 75 F to 130 F as a result of the above exposure.

(3) The weld metal and heat affected zone (HAZ) materials exhibited the largest shift in RT<sub>NDT</sub>. However, because the intermediate shell plate material has a high initial (unirradiated) RT<sub>NDT</sub>, it will control the heatup and cooldown limitations at least until the next surveillance capsule is removed.

(4) The estimated maximum neutron fluence of  $6.92 \times 10^{17}$  neutrons/cm<sup>2</sup> > 1 MeV received by the vessel wall accrued in 1.27 full power years. Therefore, the projected maximum neutron fluence after 32 effective full power years (EFPY) is  $1.74 \times 10^{19}$  neutrons/cm<sup>2</sup> > 1 MeV. This estimate is based on a lead factor of 2.6 between Capsule T and the point of maximum pressure vessel flux.

(5) Based on Regulatory Guide 1.99 trend curves, the projected maximum shift in ductile-brittle transition temperature of the Donald C. Cook Unit 1 vessel core beltline plates at the 1/4T and 3/4T positions after 12 EFPY of operation are 110 F and 50 F, respectively. These values were used as the bases for computing heatup and cooldown limit curves for up to 12 EFPY of operation.



(6) The maximum shifts in the transition temperature of the Donald C. Cook unit 1 vessel core beltline plates at the 1/4T and 3/4T positions after 32 EFPY of operation are projected to be 180 F and 83 F, respectively.

(7) Since the weld metal and HAZ beltline materials are more sensitive to radiation embrittlement than the intermediate shell plate material, the operating limitations may come under control of the weld metal and HAZ material late in the 32 EFPY design life of the plant.

(8) The Donald C. Cook Unit No. 1 vessel plates, weld metal and HAZ material located in the core beltline region are projected to retain sufficient toughness to meet the current requirements of 10CFR50 Appendix G throughout the design life of the unit.

## II. BACKGROUND

The allowable loadings on nuclear pressure vessels are determined by applying the rules in Appendix G, "Fracture Toughness Requirements," of 10CFR50.(1)\* In the case of pressure-retaining components made of ferritic materials, the allowable loadings depend on the reference stress intensity factor ( $K_{IR}$ ) curve indexed to the reference nil ductility temperature ( $RT_{NDT}$ ) presented in Appendix G, "Protection Against Non-ductile Failure," of Section III of the ASME Code.(2) Further, the materials in the beltline region of the reactor vessel must be monitored for radiation-induced changes in  $RT_{NDT}$  per the requirements of Appendix H, "Reactor Vessel Material Surveillance Program Requirements," of 10CFR50.

The  $RT_{NDT}$  is defined in paragraph NB-2331 of Section III of the ASME Code as the highest of the following temperatures:

- (1) Drop-weight Nil Ductility Temperature (DW-NDT) per ASTM E 208;(3)
- (2) 60 deg F below the 50 ft-lb Charpy V-notch ( $C_V$ ) temperature;
- (3) 60 deg F below the 35 mil  $C_V$  temperature.

The  $RT_{NDT}$  must be established for all materials, including weld metal and heat affected zone (HAZ) material as well as base plates and forgings, which comprise the reactor coolant pressure boundary.

It is well established that ferritic materials undergo an increase in strength and hardness and a decrease in ductility and toughness when exposed to neutron fluences in excess of  $10^{17}$  neutrons per  $cm^2$  ( $E > 1$  MeV).(4) Also, it has been established that tramp elements, particularly copper and

---

\* Superscript numbers refer to references at the end of the text.

phosphorous, affect the radiation embrittlement response of ferritic materials.<sup>(5-7)</sup> The relationship between increase in  $RT_{NDT}$  and copper content is not defined completely. For example, Regulatory Guide 1.99, originally issued in July 1975, proposed an adjustment to  $RT_{NDT}$  proportional to the square root of the neutron fluence. Westinghouse Electric Corporation, in their comments on the 1975 issue of Regulatory Guide 1.99<sup>(8)</sup>, believed that the proposed relationship overestimates the shift at fluences greater than  $1.9 \times 10^{19}$  and underestimates the shift at fluences less than  $1.9 \times 10^{19}$ . On the other hand, Combustion Engineering, in their comments on the 1975 issue of Regulatory Guide 1.99<sup>(9)</sup>, suggested that the proposed relationship is overly conservative at fluences below  $10^{19}$  neutrons per  $cm^2$  ( $E > 1$  MeV). There is also disagreement concerning the prediction of  $C_v$  upper shelf response to exposure to neutron irradiation.<sup>(7-9)</sup> After reviewing the comments and evaluating additional surveillance program data, the NRC issued a revision to Regulatory Guide 1.99 which raised the upper limit of the transition temperature adjustment curve. In this report, estimates of shifts in  $RT_{NDT}$  are based on Revision 1 of Regulatory Guide 1.99<sup>(7)</sup>, issued in April 1977.

In general, the only ferritic pressure boundary materials in a nuclear plant which are expected to receive a fluence sufficient to affect  $RT_{NDT}$  are those materials which are located in the core beltline region of the reactor pressure vessel. Therefore, material surveillance programs include specimens machined from the plate or forging material and weldments which are located in such a region of high neutron flux density. ASTM E 185<sup>(10)</sup> describes the current recommended practice for monitoring and evaluating the radiation-induced changes occurring in the mechanical properties of pressure vessel beltline materials.

Westinghouse has provided such a surveillance program for the Donald C. Cook Unit No. 1 nuclear power plant. The encapsulated  $C_v$  specimens are located near the O.D. surface of the thermal shield at a point where the fast neutron flux density is about three times that at the adjacent vessel wall surface. Therefore, the increases (shifts) in transition temperatures of the materials in the pressure vessel are generally less than the corresponding shifts observed in the surveillance specimens. However, because of azimuthal variations in neutron flux density, capsule fluences may lead or lag the maximum vessel fluence in a corresponding exposure period. For example, Capsule T (removed during the 1977 refuelling outage) was exposed to a neutron fluence approximately 2.6 times that at the maximum exposure point on the vessel I.D., while Capsule X (scheduled for removal at a later date) is being exposed to a neutron flux about 60% of that at the point of maximum vessel exposure. The capsules also contain several dosimeter materials for experimentally determining the average neutron flux density at each capsule location during the exposure period.

The Donald C. Cook Unit No. 1 material surveillance capsules also include tensile specimens as recommended by ASTM E 185. At the present time, irradiated tensile properties are used primarily to indicate that the materials tested continue to meet the requirements of the appropriate material specification. In addition, the degree of radiation hardening indicated by the tensile yield strength is used to judge the credibility of the surveillance data.<sup>(7)</sup>

Wedge opening loading (WOL) fracture mechanics specimens, machined from plate material and weld metal, are also contained in the capsules. Current technology limits the testing of these specimens at temperatures well below

the minimum service temperature to obtain valid fracture mechanics data per ASTM E 399<sup>(11)</sup>, "Standard Method of Test for Plane-Strain Fracture Toughness of Metallic Materials." However, recent work reported by Mager and Witt<sup>(12)</sup> may lead to methods for evaluating high-toughness materials with small fracture mechanics specimens. Currently, the NRC suggests storing these specimens until an acceptable testing procedure has been defined.

This report describes the results obtained from testing the contents of Capsule T. These data are analyzed to estimate the radiation-induced changes in the mechanical properties of the pressure vessel at the time of the 1977 refuelling outage as well as predicting the changes expected to occur at selected times in the future operation of the Donald C. Cook Unit No. 1 power plant.

### III. DESCRIPTION OF MATERIAL SURVEILLANCE PROGRAM

The Donald C. Cook Unit No. 1 material surveillance program is described in detail in WCAP 8047<sup>(13)</sup>, dated March 1973. Eight materials surveillance capsules were placed in the reactor vessel between the thermal shield and the vessel wall prior to startup, see Figure 1. The vertical center of each capsule is opposite the vertical center of the core. The neutron flux density at the Capsule T location leads the maximum flux density on the vessel I.D. by a factor of 2.6.<sup>(13)</sup> The capsules each contain Charpy V-notch, tensile and WOL specimens machined from the SA533 Gr B plate, weld metal and heat affected zone (HAZ) materials located at the core beltline plus Charpy V-notch specimens machined from a reference heat of steel utilized in a number of Westinghouse surveillance programs.

The chemistries and heat treatments of the vessel surveillance materials are summarized in Table I. All test specimens were machined from the test materials at the quarter-thickness ( $1/4 T$ ) location after performing a simulated postweld stress-relieving treatment. Weld and HAZ specimens were machined from a stress-relieved weldment which joined sections of the intermediate shell course. HAZ specimens were obtained from the plate B4406-3 side of the weldment. The longitudinal base metal  $C_v$  specimens were oriented with their long axis parallel to the primary rolling direction and with V-notches perpendicular to the major plate surfaces. The transverse base metal  $C_v$  specimens were oriented with their long axis perpendicular to the primary rolling direction and with V-notches perpendicular to the major plate surfaces. Tensile specimens were machined with the longitudinal axis parallel to the plate rolling direction. The WOL specimens were machined

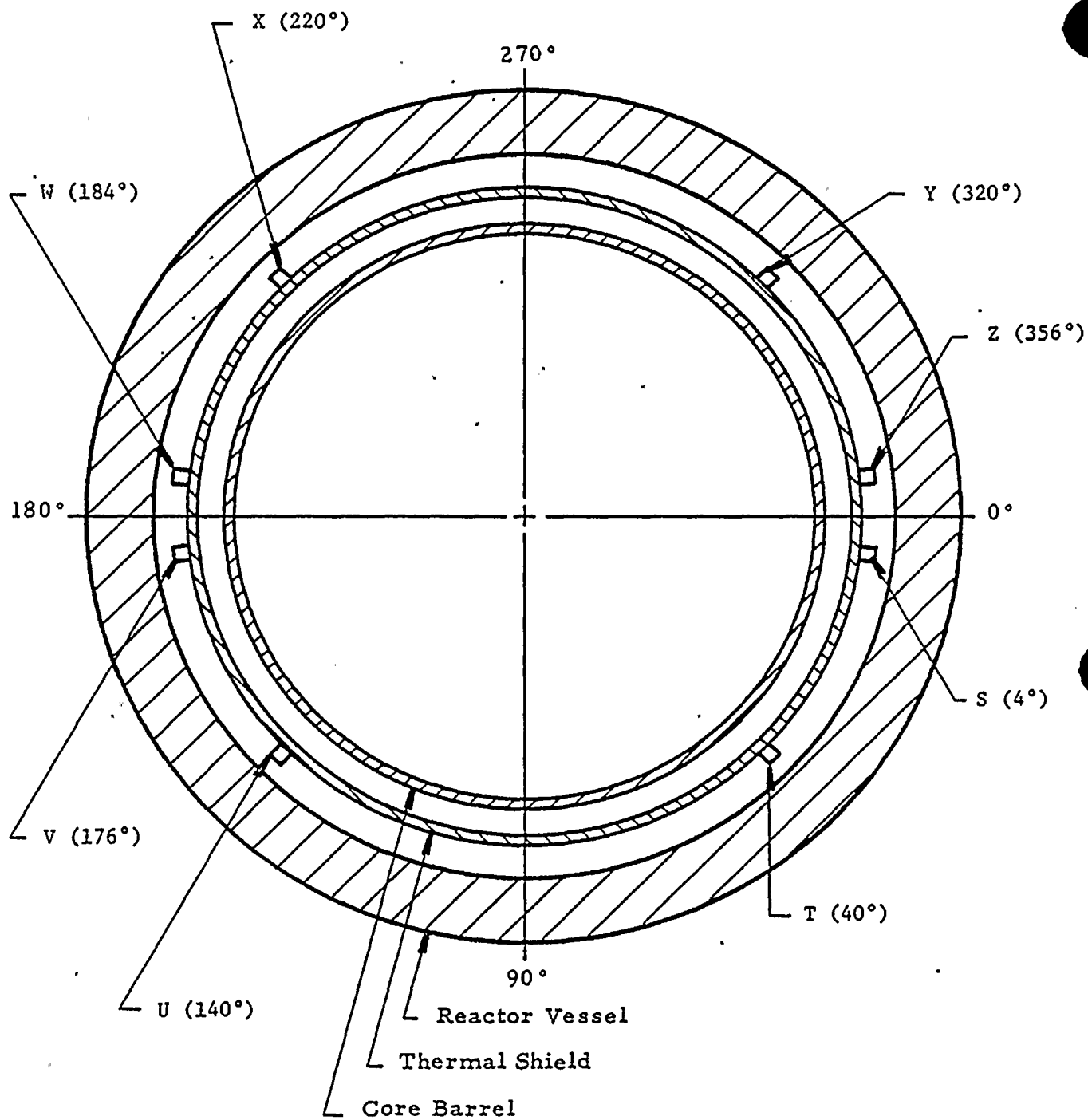


FIGURE 1. ARRANGEMENT OF SURVEILLANCE CAPSULES  
IN THE PRESSURE VESSEL

TABLE I

DONALD C. COOK UNIT NO. 1 REACTOR VESSEL SURVEILLANCE MATERIALS(13)

Heat Treatment History

Shell Plate Material:

Heated to 1600 F for 4 hours, water quenched.

Tempered at 1225 F for 4 hours, air cooled.

Stress relieved at 1150 F for 40 hours, furnace cooled.

Weldment:

Stress relieved at 1150 F for 40 hours, furnace cooled.

Correlation Monitor:

1675 F, 4 hours, air cooled.

1650 F, 4 hours, water quenched.

1225 F, 4 hours, furnace cooled

1150 F, 40 hours, furnace cooled to 600 F.

Chemical Composition (Percent)

<u>Material</u>	<u>C</u>	<u>Mn</u>	<u>P</u>	<u>S</u>	<u>Si</u>	<u>Ni</u>	<u>Mo</u>	<u>Cu</u>
Plate B4406-3	0.24	1.40	0.009	0.015	0.25	0.49	0.46	0.14
Weld Metal	0.26	1.33	0.023	0.014	0.18	0.74	0.44	0.27
Correlation Monitor	0.22	1.48	0.012	0.018	0.25	0.68	0.52	0.14



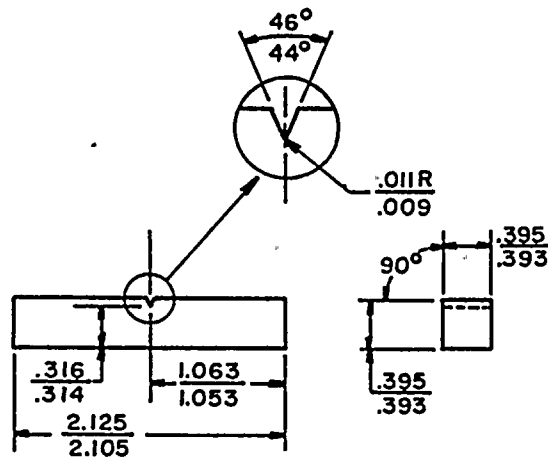
with the simulated crack perpendicular to both the primary rolling direction and to the major plate surfaces. All mechanical test specimens, see Figure 2, were taken at least one plate thickness from the quenched edges of the plate material.

Capsule T contained 44 Charpy V-notch specimens (10 longitudinal and 10 transverse from the plate material, plus 8 each from weld metal, HAZ and the reference steel plate); 4 tensile specimens (2 plate and 2 weld metal); and 4 WOL specimens (2 plate and 2 weld metal). The specimen numbering system and location within Capsule T is shown in Figure 3.

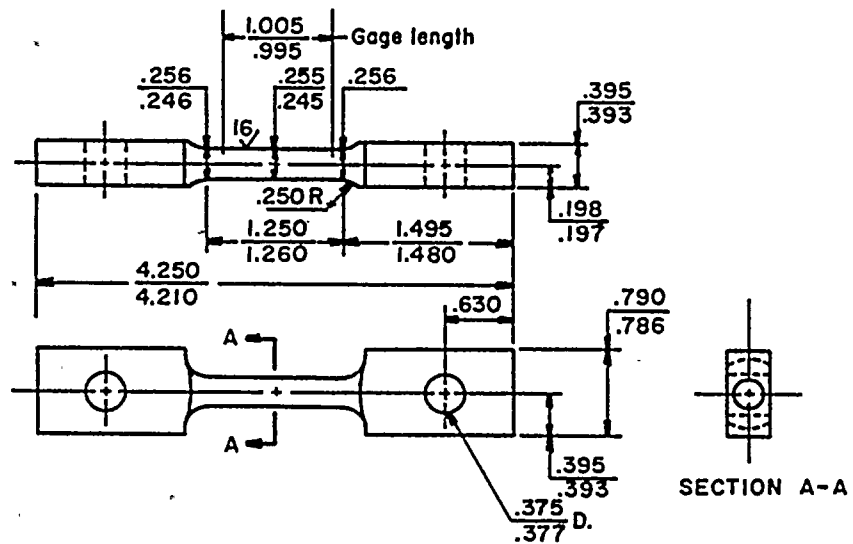
Capsule T also was reported to contain the following dosimeters for determining the neutron flux density:

Target Element	Form	Quantity
Iron	Bare wire	5
Copper	Bare wire	3
Nickel	Bare wire	3
Cobalt (in aluminum	Bare wire	2
Cobalt (in aluminum)	Cd shielded wire	.2
Uranium-238	Cd shielded oxide	1
Neptunium-237	Cd shielded oxide	1

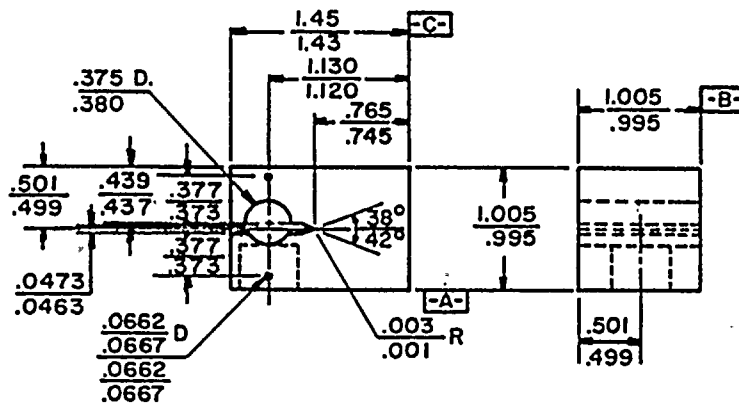
Two eutectic alloy thermal monitors had been inserted in holes in the steel spacers in Capsule T. One (located at the bottom) was 2.5% Ag and 97.5% Pb with a melting point of 579 F. The other (located at the top of the capsule) was 1.75% Ag, 0.75% Sn and 97.5% Pb having a melting point of 590 F.



(a) Charpy V-notch Impact Specimen



(b) Tensile Specimen



(c) Wedge Opening Loading Specimen

FIGURE 2. VESSEL MATERIAL SURVEILLANCE SPECIMENS

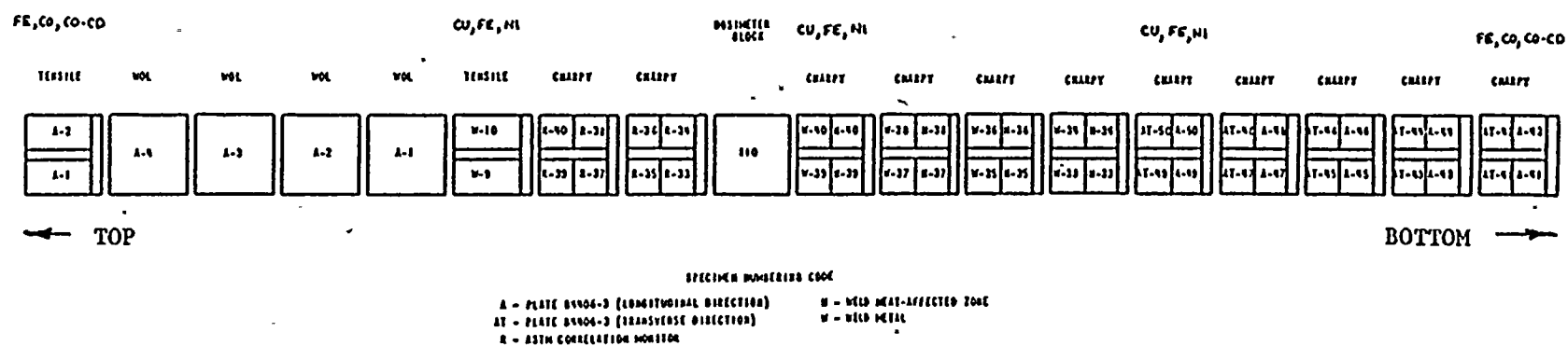


FIGURE 3. ARRANGEMENT OF SPECIMENS AND DOSIMETERS IN CAPSULE T

#### IV. TESTING OF SPECIMENS FROM CAPSULE T

The capsule shipment, capsule opening, specimen testing and reporting of results were carried out in accordance with the Project Plan for Donald C. Cook Unit No. 1 Reactor Vessel Irradiation Surveillance Program. The SwRI Nuclear Projects Operating Procedures called out in this plan include:

- (1) XI-MS-1, "Determination of Specific Activity of Neutron Radiation Detector Specimen."
- (2) XI-MS-3, "Conducting Tension Tests on Metallic Materials."
- (3) XI-MS-4, "Charpy Impact Tests on Metallic Materials."
- (4) XIII-MS-1, "Opening Radiation Surveillance Capsules and Handling and Storing Specimens."
- (5) XI-MS-5, "Conducting Wedge-Opening-Loading Tests on Metallic Materials."
- (6) XI-MS-6, "Determination of Specific Activity of Neutron Radiation Fission Monitor Detector Specimens."

Copies of the above documents are on file at SwRI.

Southwest Research Institute utilized a procedure which had been prepared for the 1977 refuelling outage for the removal of Capsule T from the reactor vessel and the shipment of the capsule to the SwRI laboratories. SwRI contracted with Todd Shipyards - Nuclear Division to supply appropriate cutting tools and a licensed shipping cask. Todd personnel severed the capsule from its extension tube, sectioned the extension tube into three-foot lengths, supervised the loading of the capsule and extension tube materials into the shipping cask, and transported the cask to San Antonio.

The capsule shell had been fabricated by making two long seam welds to join two half-shells together. The long seam welds were milled off on a Bridgeport vertical milling machine set up in one hot cell. Before milling off the long seam weld beads, transverse saw cuts were made to remove the two capsule ends. After the long seam welds had been milled away, the top half of the capsule shell was removed. The specimens and spacer blocks were carefully removed and placed in an indexed receptacle so that capsule location was identifiable. After the disassembly had been completed, the specimens were carefully checked for identification and location, as listed in WCAP 8047.(13)

Each specimen was inspected for identification number, which was checked against the master list in WCAP 8047. No discrepancies were found. The thermal monitors and dosimeter wires were removed from the holes in the spacers. The thermal monitors, contained in quartz vials, were examined, and no evidence of melting was observed, thus indicating that the maximum temperature during exposure of Capsule T did not exceed 579 F.

The specific activities of the dosimeters were determined at SwRI with an NDC 2200 multichannel analyzer and an NaI(Th) 3 x 3 scintillation crystal. The calibration of the equipment was accomplished with appropriate standards and an interlaboratory cross check with two independent counting laboratories on  $^{60}\text{Co}$ -,  $^{54}\text{Mn}$ - and  $^{58}\text{Co}$ -containing dosimeter wires. All activities were corrected to the time-of-removal (TOR) at reactor shutdown. Infinitely dilute saturated activities ( $A_{\text{SAT}}$ ) were calculated for each of the dosimeters because  $A_{\text{SAT}}$  is directly related to the product of the

energy-dependent microscopic activation cross section and the neutron flux density. The relationship between  $A_{TOR}$  and  $A_{SAT}$  is given by:

$$\frac{A_{TOR}}{A_{SAT}} = \sum_{m=1}^{m=n} (1 - e^{-\lambda T_m}) (e^{-\lambda t_m}) \quad (1)$$

where:  $m$  = operating period;  
 $\lambda$  = decay constant for the activation product, day<sup>-1</sup>;  
 $T_m$  = equivalent operating days at 3250 MwTh for operating period  $m$ ;  
 $t_m$  = decay time after operating period  $m$ , days.

The Donald C. Cook Unit No. 1 operating history up to the 1977 refuelling outage is presented in Table II. The specific activity at time of removal (TOR) and the specific saturated activity calculated for each dosimeter are presented in Table III.

The primary result desired from the dosimeter analysis is the total fast neutron fluence (> 1 MeV) which the surveillance specimens received. The average flux density at full power is given by:

$$\phi = \frac{A_{SAT}}{N_0 \bar{\sigma}} \quad (2)$$

where:  $\phi$  = energy-dependent neutron flux density, n/cm<sup>2</sup>-sec;  
 $A_{SAT}$  = saturated activity, dps/mg target element;  
 $\bar{\sigma}$  = spectrum-averaged activation cross section, cm<sup>2</sup>;  
 $N_0$  = number of target atoms per mg.

The total neutron fluence is then equal to the product of the average neutron flux density and the equivalent reactor operating time at full power.

TABLE II

SUMMARY OF REACTOR OPERATIONS  
DONALD C. COOK UNIT NO. 1

Operating Period	Dates		Operating Days	Shutdown Days	Power Generation (MWD <sub>t</sub> )	Equivalent Operating Days (T <sub>m</sub> )	Decay Time After Period (t <sub>m</sub> )
	Start	Stop					
1	2/2/75	2/14/75	13	-	2,194	0.68	678
	2/15/75	2/16/75	-	2	-	-	-
2	2/17/75	2/17/75	1	-	228	0.07	675
	2/18/75	2/20/75	-	3	-	-	-
3	2/21/75	3/18/75	26	-	29,604	9.11	646
	3/19/75	4/3/75	-	16	-	-	-
4	4/4/75	6/24/75	82	-	200,616	61.73	548
	6/25/75	6/26/75	-	2	-	-	-
5	6/27/75	7/3/75	7	-	15,432	4.75	539
	7/4/75	7/22/75	-	19	-	-	-
6	7/23/75	10/11/75	81	-	201,506	62.00	439
	10/12/75	10/14/75	-	3	-	-	-
7	10/15/75	10/31/75	17	-	40,163	12.35	419
	11/1/75	11/14/75	-	14	-	-	-
8	11/15/75	1/1/76	48	-	116,552	35.86	357
	1/2/76	1/4/76	-	3	-	-	-
9	1/5/76	4/12/76	99	-	256,178	78.82	255
	4/13/76	5/9/76	-	27	-	-	-
10	5/10/76	7/1/76	53	-	143,868	44.27	175
	7/2/76	7/5/76	-	4	-	-	-
11	7/6/76	9/10/76	67	-	205,682	63.29	104
	9/11/76	9/18/76	-	8	-	-	-
12	9/19/76	11/20/76	63	-	196,520	60.47	33
	11/21/76	11/21/76	-	1	-	-	-
13	11/22/76	12/23/76	32	-	92,754	28.54	0
Total, Cycle 1					1,501,297	461.94	

TABLE III

SUMMARY OF NEUTRON DOSIMETRY RESULTS  
DONALD C. COOK UNIT NO. 1--CAPSULE T

Monitor Identification	Activation Reaction	ATOR (dps/mg)	ASAT (dps/mg)
Fe - Top	$^{54}\text{Fe}(n,p)^{54}\text{Mn}$	$1.93 \times 10^3$	$3.34 \times 10^3$
Fe - Top Mid.	"	$1.69 \times 10^3$	$2.94 \times 10^3$
Fe - Mid.	"	$1.69 \times 10^3$	$2.93 \times 10^3$
Fe - Bot. Mid.	"	$1.69 \times 10^3$	$2.93 \times 10^3$
Fe - Bot.	"	$1.80 \times 10^3$	$3.11 \times 10^3$
	Average	$1.76 \times 10^3$	$3.05 \times 10^3$
Cu - Top Mid.	$^{63}\text{Cu}(n,\alpha)^{60}\text{Co}$	$5.14 \times 10^1$	$3.43 \times 10^2$
Cu - Mid.	"	$5.27 \times 10^1$	$3.52 \times 10^2$
Cu - Bot. Mid.	"	$6.04 \times 10^1$	$4.03 \times 10^2$
Ni - Top Mid.	$^{58}\text{Ni}(n,p)^{58}\text{Co}$	$3.83 \times 10^4$	$4.46 \times 10^4$
Ni - Mid.	"	$3.77 \times 10^4$	$4.38 \times 10^4$
Ni - Bot. Mid.	"	$3.95 \times 10^4$	$4.59 \times 10^4$
Co - Top	$^{59}\text{Co}(n,\gamma)^{60}\text{Co}$	$4.87 \times 10^6$	$3.25 \times 10^7$
Co(Cd) - Top	"	$1.83 \times 10^6$	$1.22 \times 10^7$
Co - Bot.	"	$5.03 \times 10^6$	$3.36 \times 10^7$
Co(Cd) - Bot.	"	$1.64 \times 10^6$	$1.09 \times 10^7$
U-238	$^{238}\text{U}(n,f)^{137}\text{Cs}$	$1.20 \times 10^3$	N/A
Np-237	$^{237}\text{Np}(n,f)^{137}\text{Cs}$	$4.53 \times 10^3$	N/A



The neutron flux density was calculated from the  $^{54}\text{Fe}(n,p)^{54}\text{Mn}$  reaction because it has a high energy threshold and the energy response is well known. The energy spectrum for Capsule T was calculated with the DOT 3.5 two-dimensional discrete ordinates transport code with a 22-group neutron cross section library, a  $P_1$  expansion of the scattering matrix and an  $S_8$  order of angular quadrature. The normalized spectrum for Capsule T and the group-organized cross sections for the  $^{54}\text{Fe}(n,p)^{54}\text{Mn}$  reaction derived from the ENDF/B-IV library<sup>(14)</sup> are given in Table IV. The value of  $\bar{\sigma}_{\text{Fe}}$  is given by:

$$\bar{\sigma}_{\text{Fe}}(> 1 \text{ MeV}) = \frac{\sum_{1.10}^{10 \text{ MeV}} \sigma_{\text{Fe}}(E) \phi(E) dE}{\sum_{1.00}^{10 \text{ MeV}} \phi(E) dE} \quad (3)$$

where:  $\bar{\sigma}_{\text{Fe}}(> 1 \text{ MeV})$  = the calculated spectrum-averaged cross section for flux  $> 1 \text{ MeV}$ ,  $\text{cm}^2$  determined for the  $^{54}\text{Fe}(n,p)^{54}\text{Mn}$  reaction.

The resulting value obtained for fast ( $> 1 \text{ MeV}$ ) neutron flux density at the Capsule T location was  $4.50 \times 10^{10}$  neutrons/ $\text{cm}^2$ -sec. Since Donald C. Cook Unit No. 1 operated for an equivalent 461.94 full power days up to the 1977 refuelling outage, the total neutron fluence for Capsule T is equal to  $1.80 \times 10^{18}$  neutrons/ $\text{cm}^2$  ( $E > 1 \text{ MeV}$ ) based on the calculated spectrum at the capsule location.

Assuming a fission-spectrum energy distribution at the capsule location, the cross-section for the  $^{54}\text{Fe}(n,p)^{54}\text{Mn}$  reaction ( $E > 1 \text{ MeV}$ ) would be 98.26 mb.<sup>(4)</sup> The resulting flux and fluence values would be  $4.95 \times 10^{10}$  neutrons/ $\text{cm}^2$ -sec and  $1.97 \times 10^{18}$  neutrons/ $\text{cm}^2$ , respectively.

TABLE IV

FAST NEUTRON SPECTRUM AND IRON ACTIVATION  
CROSS SECTIONS FOR CAPSULE T

<u>Energy Range (MeV)</u>	<u>Normalized Neutron Flux</u>	<u><math>^{54}\text{Fe}(n,p)^{54}\text{Mn}</math> Cross Section (barns)</u>
8.18 - 10.0	0.0098	0.581
6.36 - 8.18	0.0254	9.577
4.96 - 6.36	0.0482	0.491
4.06 - 4.96	0.0471	0.354
3.01 - 4.06	0.0855	0.205
2.35 - 3.01	0.1400	0.099
1.83 - 2.35	0.1752	0.023
1.11 - 1.83	0.4689	0.0014

$$\bar{\sigma}_{\text{Fe}} = 0.108 \text{ barns}$$

The irradiated Charpy V-notch specimens were tested on a SATEC impact machine. The test temperatures were selected to develop the ductile-brittle transition and upper shelf regions. The unirradiated Charpy V-notch impact data reported by Westinghouse<sup>(13)</sup> and the data obtained by SwRI on the specimens contained in Capsule T are presented in Tables V through IX. The Charpy V-notch transition curves for the three plate materials and the correlation monitor material are presented in Figures 4 through 8. The radiation-induced shift in transition temperatures for the vessel plates are indicated at 50 ft-lb and 35 mil lateral expansion. A summary of the shifts in  $RT_{NDT}$  and  $C_V$  upper shelf energies for each material are presented in Table X.

Tensile tests were carried out in the SwRI hot cells using a Dillon 10,000-lb capacity tester equipped with a strain gage extensometer, load cell and autographic recording equipment. One each plate and weld metal tensile specimens was tested at room temperature (RT) and at 550 F. The results, along with tensile data reported by Westinghouse on the unirradiated materials<sup>(13)</sup>, are presented in Table XI. The load-strain records are included in Appendix A.

Testing of the WOL specimens was deferred at the request of American Electric Power Service Corporation. The specimens are in storage at the SwRI radiation laboratory.

The Charpy V-notch results indicate that the HAZ is more sensitive to radiation embrittlement than the as-rolled and heat-treated plate and about equal to that of the weld metal. This is surprising because the copper content of HAZ is reported to be much lower than that of the weld metal.<sup>(13)</sup>

TABLE V

CHARPY V-NOTCH IMPACT DATA  
 THE DONALD C. COOK UNIT NO. 1 REACTOR PRESSURE VESSEL  
 INTERMEDIATE SHELL PLATE B4406-3  
 (LONGITUDINAL DIRECTION)

<u>Condition</u>	<u>Spec. No.</u>	<u>Test Temp. (°F)</u>	<u>Impact Energy (ft-lb)</u>	<u>Shear (%)</u>	<u>Lateral Expansion (mils)</u>
Baseline ↓	(a) ↓	-40	10	6	13
		-40	11	3	10
		-40	11.5	2	11
		10	24.5	9	24
		10	33	11	29
		10	31.5	13	28
		40	57	23	49
		40	42	25	40
		40	65	29	54
		76	82	45	67
		76	70	37	60
		76	78	37	61
		110	93.5	52	72
		110	100	59	77
		110	88	52	72
		160	110	95	84
		160	131.5	100	95
		160	115.5	95	83
		210	120	100	89
		210	144	100	98
		210	125	100	95
Capsule T ↓	A-44 A-45 A-49 A-50 A-41 A-47 A-42 A-48 A-43 A-46	10	10.5	1	10
		40	29	5	24
		82	38	20	31
		110	46.5	35	38
		135	62.5	25	53
		160	84	55	58
		185	99	95	80
		210	105	95	83
		250	110	100	89
		300	105.5	100	89

(a) Not reported.

TABLE VI

CHARPY V-NOTCH IMPACT DATA  
 THE DONALD C. COOK UNIT NO. 1 REACTOR PRESSURE VESSEL  
 INTERMEDIATE SHELL PLATE B4406-3  
 (TRANSVERSE DIRECTION)

<u>Condition</u>	<u>Spec. No.</u>	<u>Test Temp. (°F)</u>	<u>Impact Energy (ft-lb)</u>	<u>Shear (%)</u>	<u>Lateral Expansion (mils)</u>
Baseline ↓	(a) ↓	-40	11	5	12
		-40	11.5	5	15
		-40	14	5	15
		10	28	14	28
		10	23	9	22
		10	30	9	26
		40	40	18	36
		40	41	23	35
		40	37	18	34
		76	83	27	56
		76	43	27	44
		76	50	32	46
		76	50	27	44
		110	84	48	71
		110	54	37	51
		110	68	41	57
		160	97	90	80
		160	77	90	71
		210	90	100	75
		210	95	100	79
		210	97	100	79
		300	100	100	83
		300	94	100	75
		300	101	100	85
Capsule T ↓	AT-44	10	6	5	8
	AT-45	40	25	5	23
	AT-49	82	35	20	30
	AT-50	110	37	30	35
	AT-41	135	49.5	25	44
	AT-47	160	57	40	47
	AT-42	185	73.5	100	63
	AT-48	210	87	100	73
	AT-43	250	87	100	71
	AT-46	300	89	100	83

(a) Not reported.

TABLE VII

CHARPY V-NOTCH IMPACT DATA  
 THE DONALD C. COOK UNIT NO. 1 REACTOR PRESSURE VESSEL  
 CORE REGION WELD METAL

<u>Condition</u>	<u>Spec. No.</u>	<u>Test Temp. (°F)</u>	<u>Impact Energy (ft-lb)</u>	<u>Shear (%)</u>	<u>Lateral Expansion (mils)</u>
Baseline ↓	(a) ↓	-140	11	0	10
		-140	21	3	19
		-140	19	3	18
		-100	23.5	18	22
		-100	29	20	26
		-100	20	11	18
		-70	45.5	24	39
		-70	51	42	47
		-70	54	32	49
		-40	63	47	52
		-40	59	34	53
		-40	69	47	60
		10	83	73	69
		10	84	71	72
		10	92	75	75
		76	114	99	88
		76	107	100	87
		76	107	100	88
		210	110	100	90
		210	112	100	87
		210	111	100	93
Capsule T ↓	W-33	-40	24.5	5	19
	W-35	10	50	20	41
	W-34	75	75.5	70	67
	W-39	82	44	20	34
	W-40	110	85	95	69
	W-37	160	75	100	66
	W-38	210	98	100	66
	W-36	300	68.5	100	66

---

(a) Not reported.

TABLE VIII

CHARPY V-NOTCH IMPACT DATA  
THE DONALD C. COOK UNIT NO. 1 REACTOR PRESSURE VESSEL  
CORE REGION WELD HEAT-AFFECTED ZONE METAL

<u>Condition</u>	<u>Spec. No.</u>	<u>Test Temp. (°F)</u>	<u>Impact Energy (ft-lb)</u>	<u>Shear (%)</u>	<u>Lateral Expansion (mils)</u>
Baseline ↓	(a) ↓	-175	5.5	0	3
		-175	7	0	5
		-175	7	0	5
		-140	16	3	12
		-140	22	5	18
		-100	30	13	25
		-100	33	14	28
		-100	45	20	40
		-70	52	21	39
		-70	47	25	35
		-70	27	14	21
		-70	30	20	24
		-40	54	55	53
		-40	71	50	50
		-40	47	43	45
		10	97	90	83
		10	89	43	67
		10	82	69	64
		76	112	100	86
		76	140	100	84
		76	131	100	82
		210	129	100	85
		210	104	100	94
		210	105	100	87
Capsule T ↓	H-33	-40	10	5	9
	H-35	10	40.5	15	30
	H-34	45	30.5	25	27
	H-39	82	52.5	25	41
	H-40	110	62.5	40	46
	H-37	160	84	100	65
	H-38	210	111.5	100	78
	H-36	300	83	100	54

(a) Not reported.

TABLE IX

CHARPY V-NOTCH IMPACT DATA  
A533 GRADE B CLASS 1 CORRELATION MONITOR MATERIAL

<u>Condition</u>	<u>Spec. No.</u>	<u>Test Temp. (°F)</u>	<u>Impact Energy (ft-lb)</u>	<u>Shear (%)</u>	<u>Lateral Expansion (mils)</u>
Baseline ↓	(a) ↓	-50	5	9	3
		-50	5	9	5
		-50	3	9	4
		-20	6.5	9	6
		-20	9	13	10
		-20	6	13	9
		10	12	23	15
		10	14.5	23	14
		10	13.5	23	14
		40	22	33	23
		40	36	29	32
		40	35	29	32
		85	58.5	43	51
		85	41.5	41	42
		85	52	42	45
		110	82.5	58	60
		110	85.5	67	71
		110	63.5	55	54
		160	108.5	84	72
		160	81	85	69
		160	109	87	79
		210	117	98	84
		210	115	98	88
		210	121	100	87
		300	125	100	87
		300	117.5	100	83
		300	127	100	84
Capsule T ↓	R-33	40	13.5	5	13
	R-37	82	18.5	10	18
	R-38	110	35	20	32
	R-39	160	55.5	40	45
	R-40	210	86.5	95	66
	R-34	300	100	100	57
	R-35	350	111	100	84
	R-36	400	96.5	100	84

(a) Not reported.



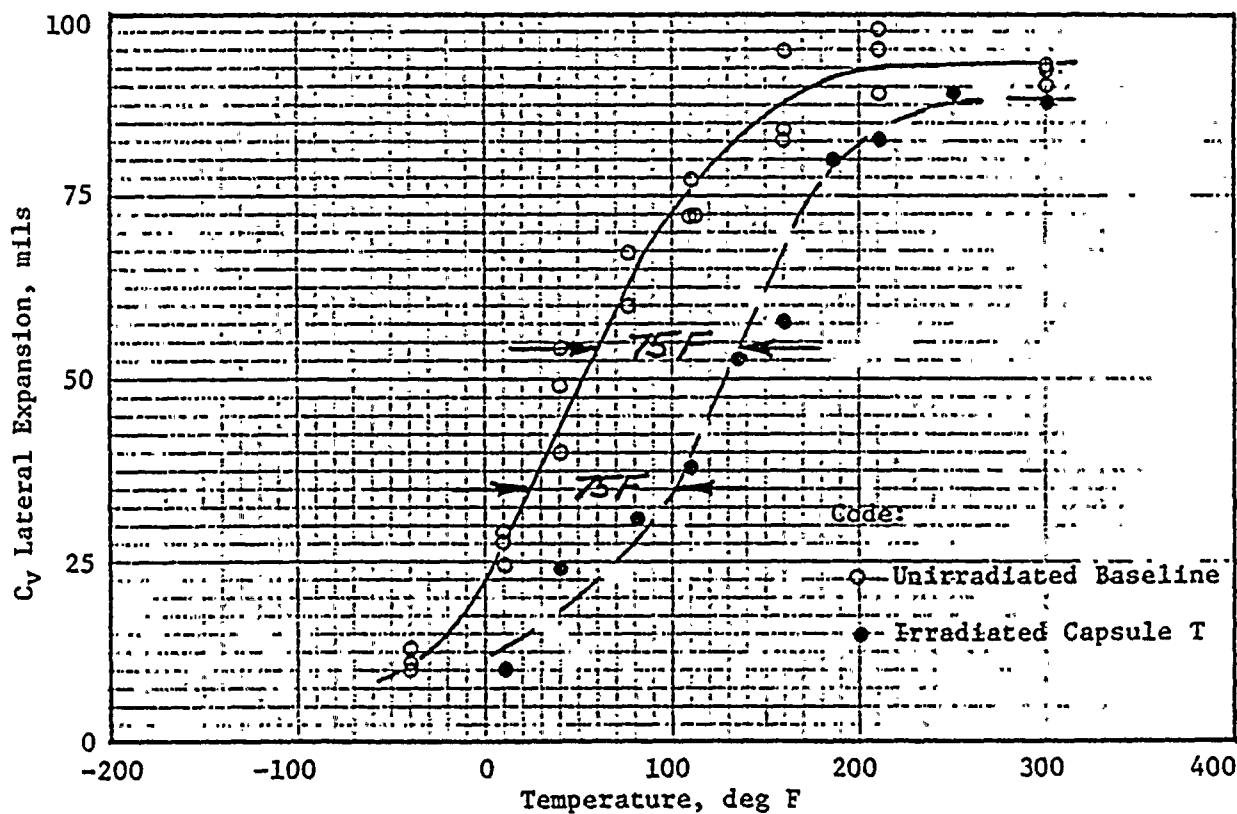
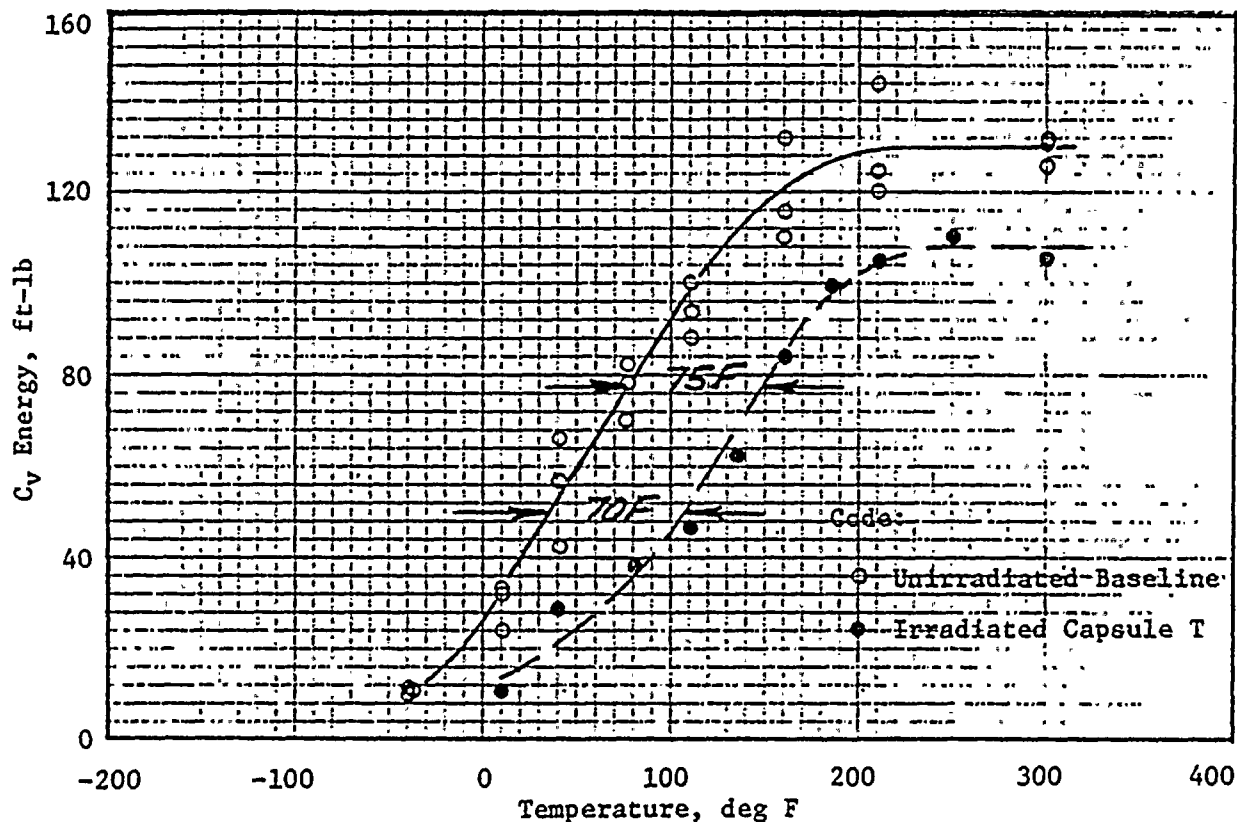


FIGURE 4. CHARPY V-NOTCH PROPERTIES OF PLATE B4406-3 (LONG.)  
DONALD C. COOK UNIT NO. 1 SURVEILLANCE PROGRAM

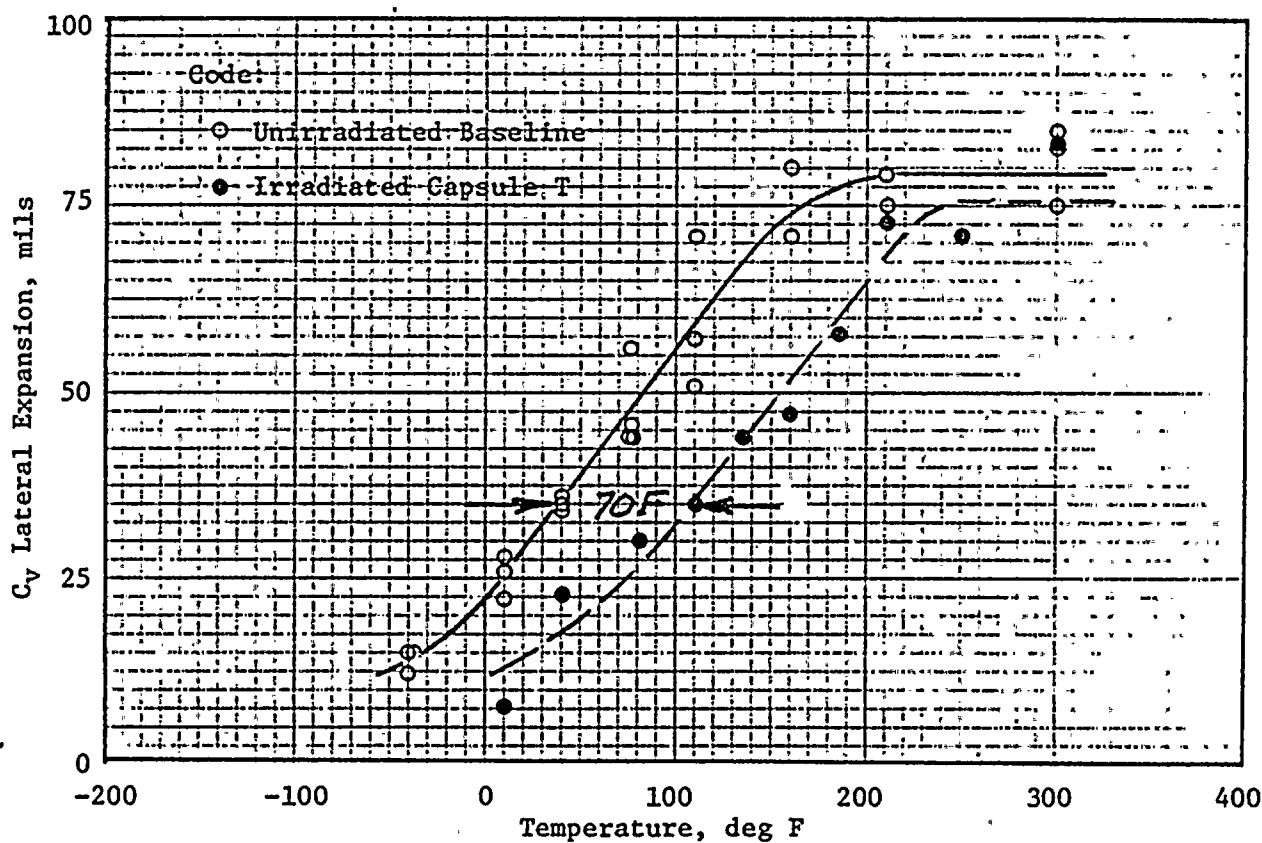
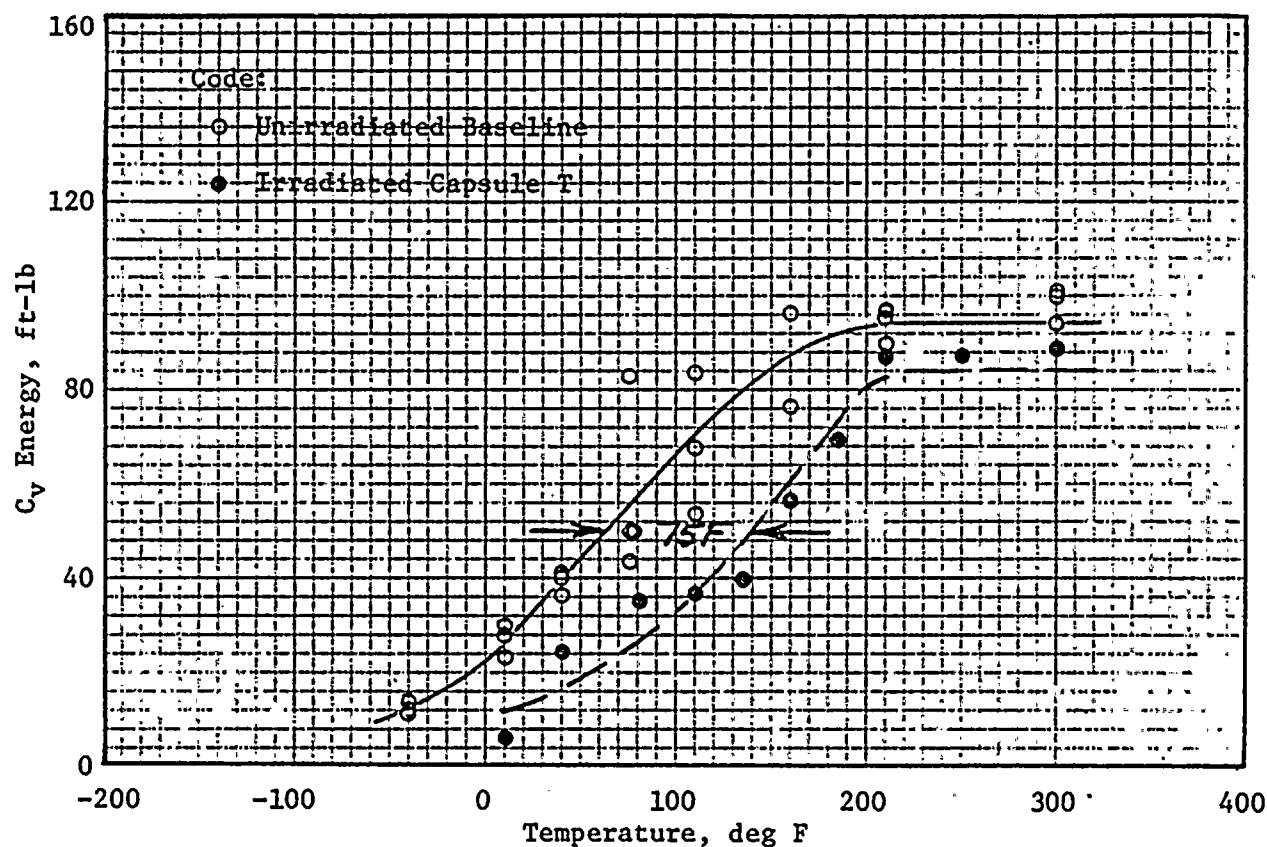


FIGURE 5. CHARPY V-NOTCH PROPERTIES OF PLATE B4406-3 (TRANS.)  
DONALD C. COOK UNIT NO. 1 SURVEILLANCE PROGRAM

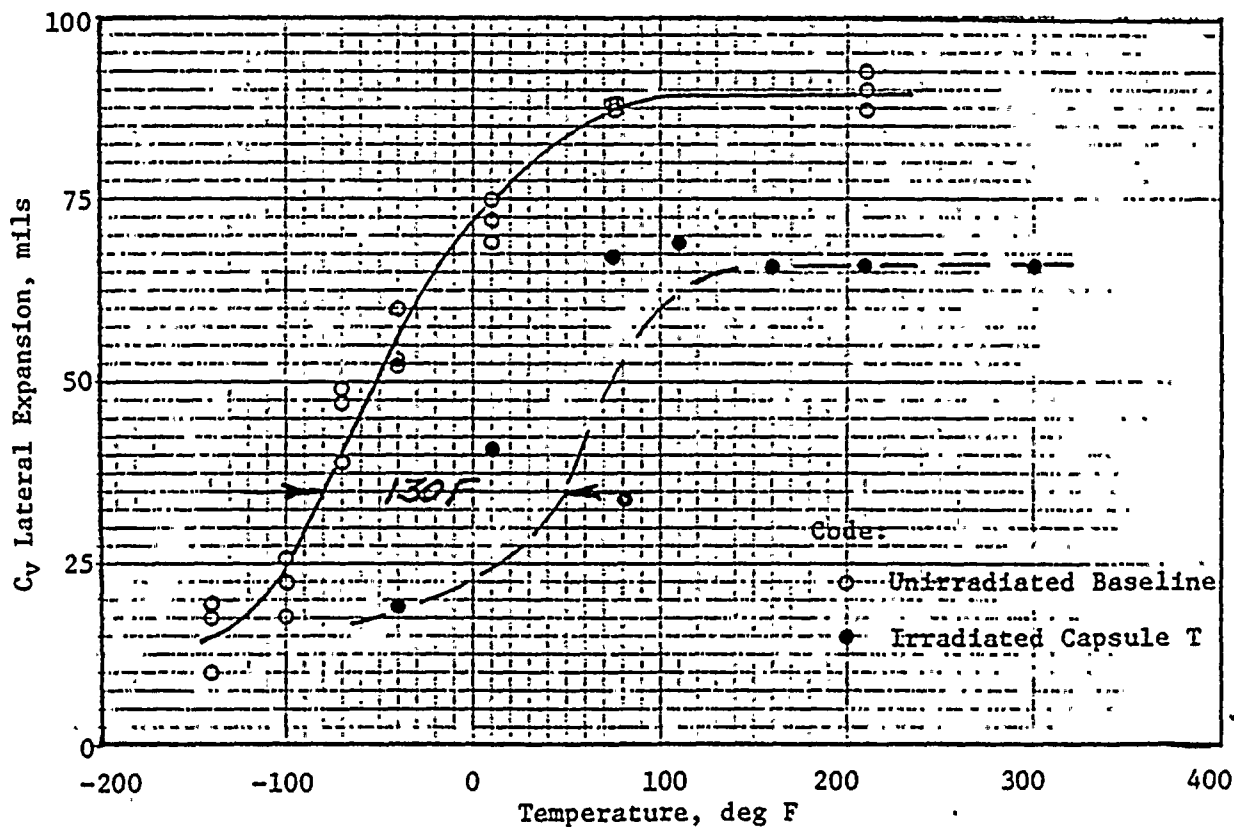
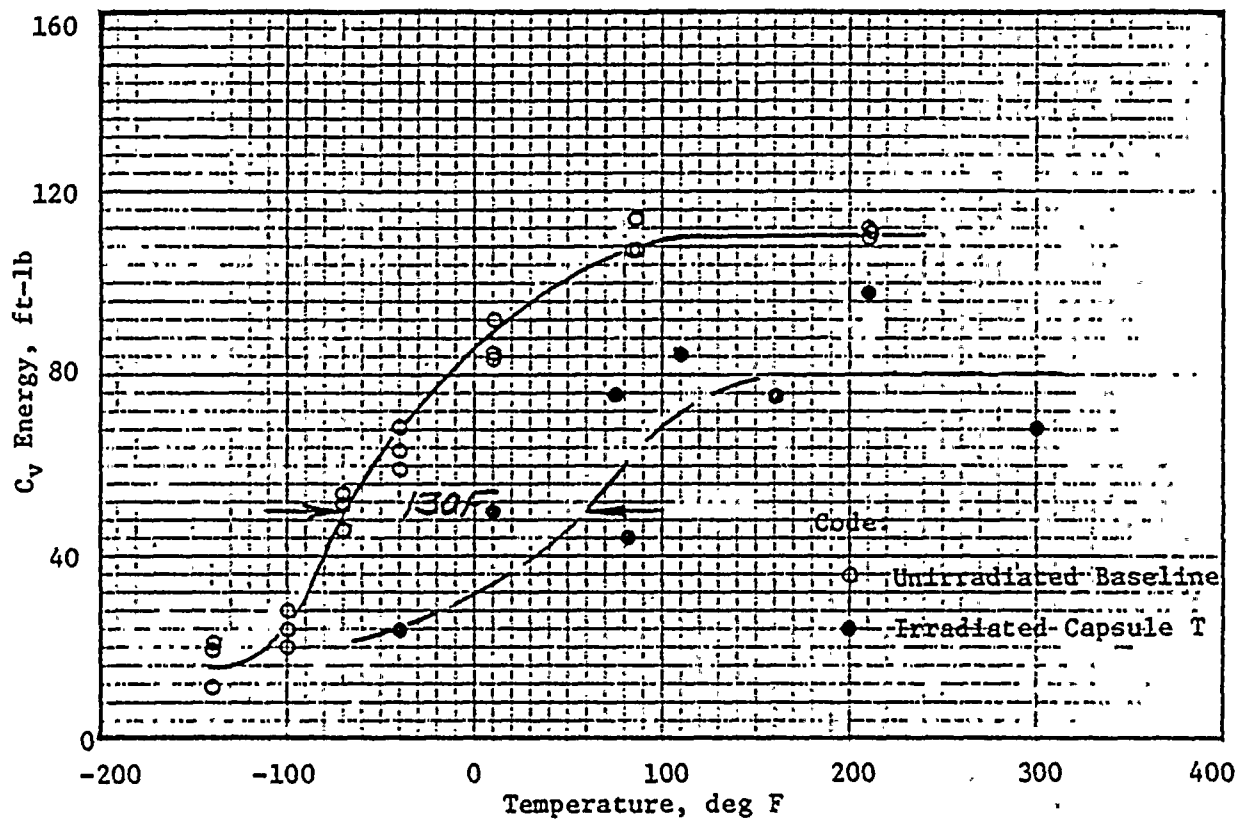


FIGURE 6. CHARPY V-NOTCH PROPERTIES OF CORE REGION WELD METAL  
DONALD C. COOK UNIT NO. 1 SURVEILLANCE PROGRAM

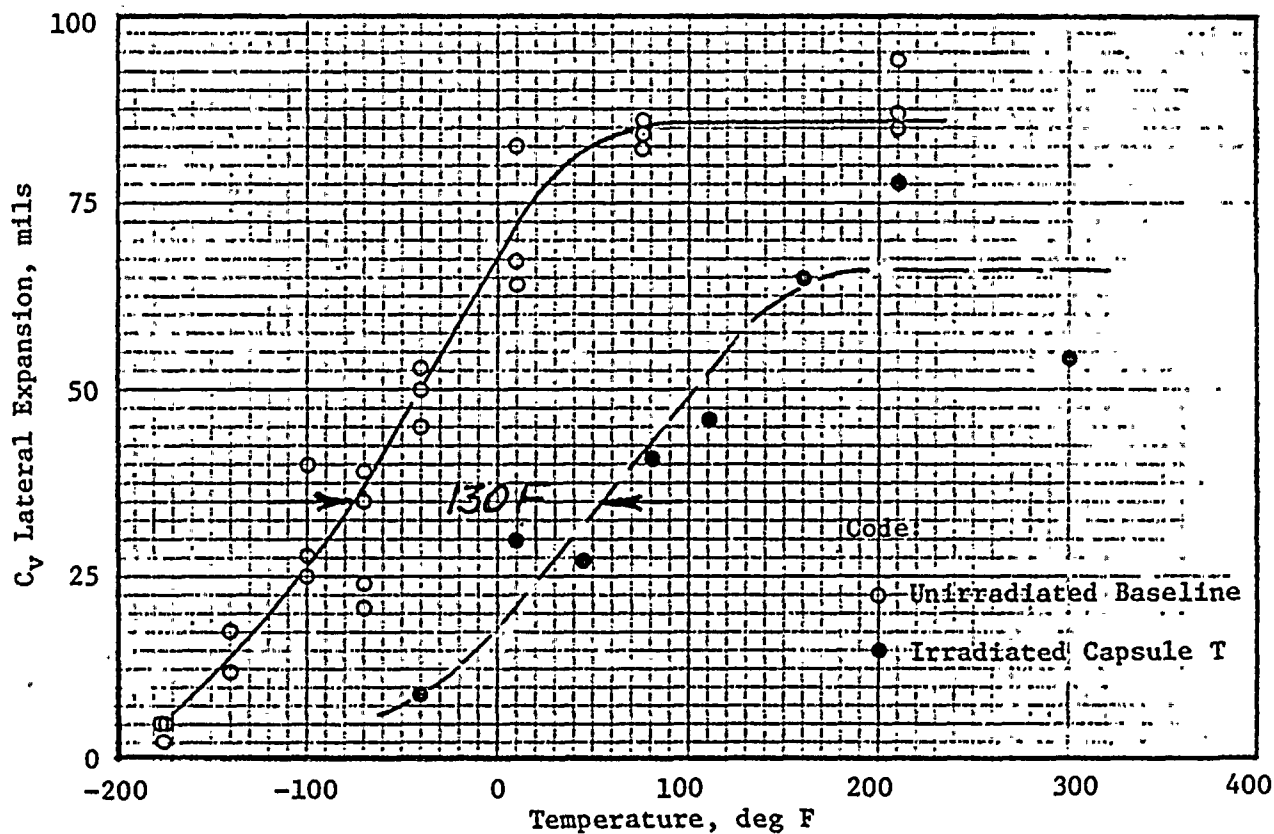
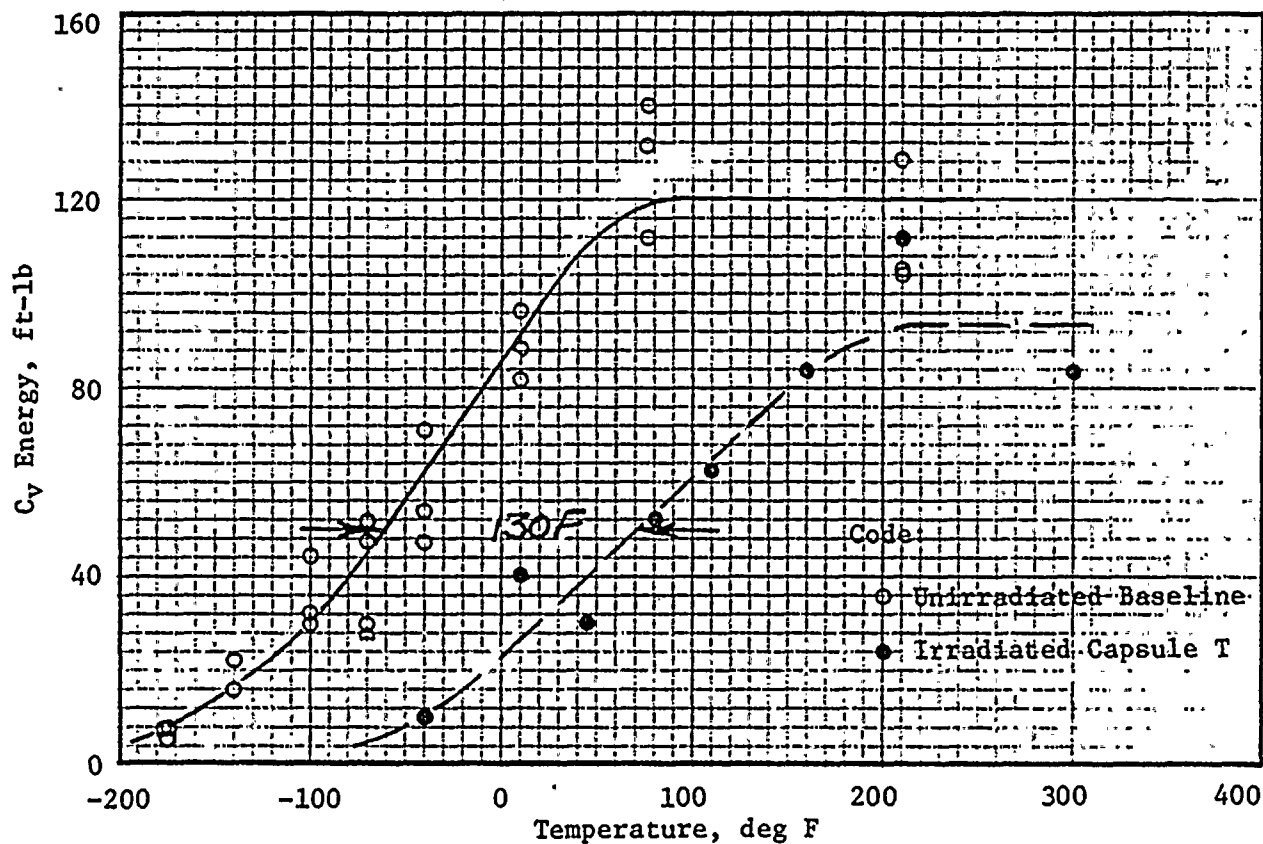


FIGURE 7. CHARPY V-NOTCH PROPERTIES OF CORE REGION HAZ MATERIAL  
DONALD C. COOK UNIT NO. 1 SURVEILLANCE PROGRAM

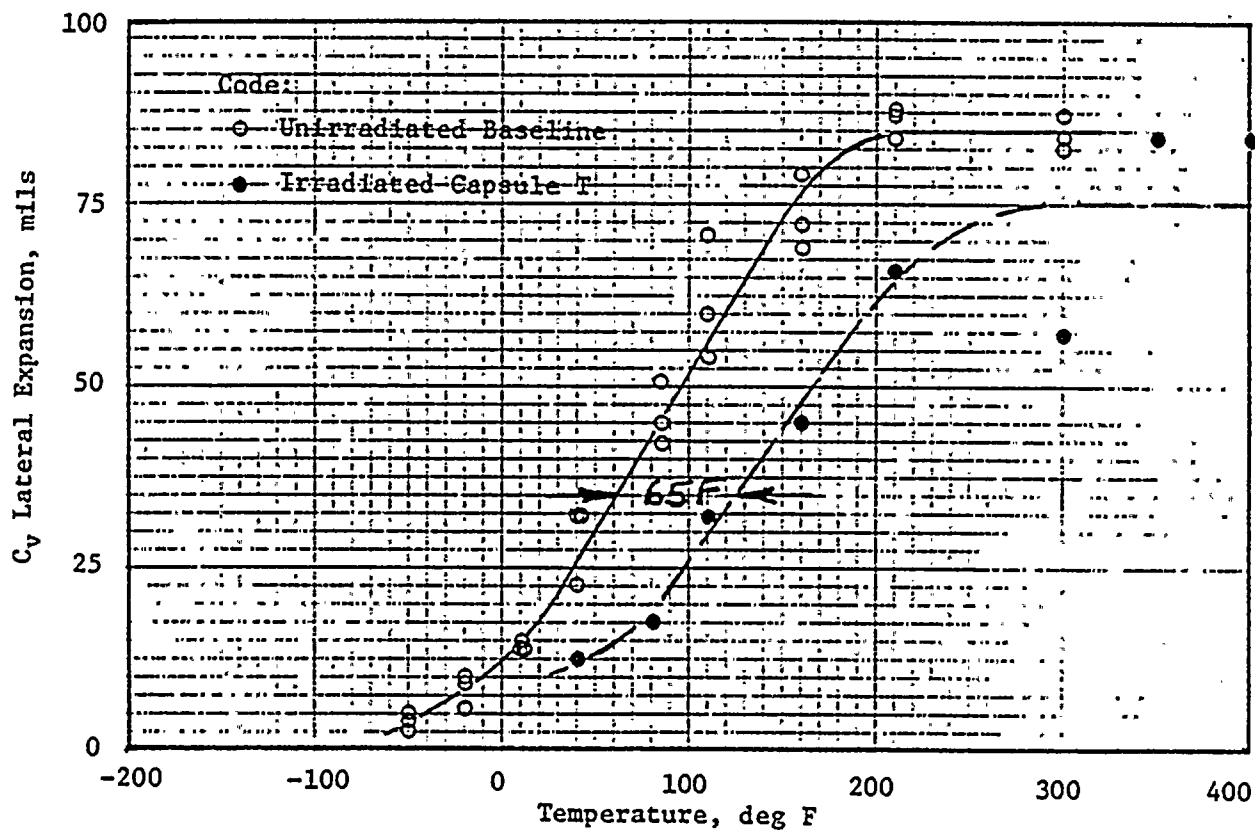
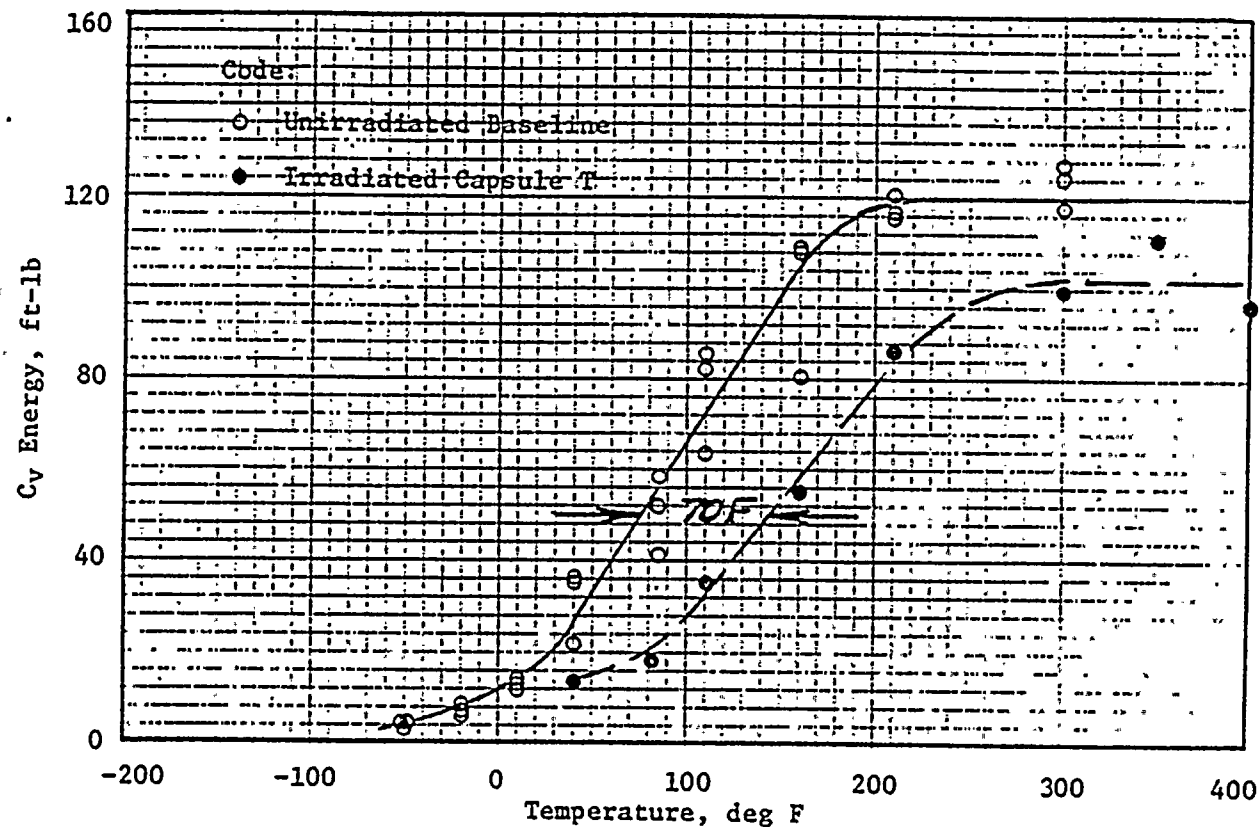


FIGURE 8. CHARPY V-NOTCH PROPERTIES OF CORRELATION MONITOR MATERIAL  
 DONALD C. COOK UNIT NO. 1 SURVEILLANCE PROGRAM

TABLE X

NOTCH TOUGHNESS PROPERTIES OF CAPSULE T SPECIMENS  
DONALD C. COOK UNIT NO. 1

	<u>Plate B4406-3</u>		<u>Weld</u>	<u>Weld</u>	<u>Correlation</u>
	<u>(Long.)</u>	<u>(Trans.)</u>	<u>Metal</u>	<u>HAZ</u>	<u>Monitor</u>
<u>50 ft-lb C<sub>v</sub> Temp. (deg F)</u>					
Irradiated	150(a)	140	60	70	145
Unirradiated	75(a)	65	-70	-60	75
$\Delta T$	75(a)	75	130	130	70
<u>35 mil C<sub>v</sub> Temp. (deg F)</u>					
Irradiated	135(b)	110	50	55	125
Unirradiated	60(b)	40	-80	-75	60
$\Delta T$	75(b)	70	130	130	65
<u>C<sub>v</sub> Upper Shelf Energy (ft-lb)</u>					
Unirradiated	130	94	110	120	120
Irradiated	108	84	80	93	102
$\Delta E$ , ft-lbs	22	10	30	27	18
$\Delta E$ , %	16.9	10.6	27.3	22.5	15

(a) Energy transition at 77 ft-lb.

(b) Lateral expansion transition at 54 mil.

TABLE XI  
TENSILE PROPERTIES OF SURVEILLANCE MATERIALS  
CAPSULE T

Condition	Specimen Ident.	Test Temp. (°F)	0.2% Yield Strength (psi)	Tensile Strength (psi)	Total Elongation (%)	Reduction in Area (%)
Baseline ↓	B4406-3 (Long.) ↓	Room	68,650	90,650	27.7	70.4
		Room	68,250	90,250	27.4	69.6
		300	61,350	82,650	23.4	69.4
		300	61,200	82,300	22.6	69.7
		600	58,000	87,000	26.0	65.1
		600	58,550	87,400	25.4	67.0
Capsule T ↓	A-1 A-2	Room	72,700	99,800	24.3	65.7
		550	66,700	93,000	20.2	64.3
Baseline ↓	B4406-3 (Trans.) ↓	Room	68,700	90,300	26.6	65.8
		Room	67,600	89,450	25.6	65.0
		300	61,000	82,800	23.0	65.0
		300	60,900	81,900	23.3	64.6
		600	58,300	86,000	24.8	58.8
		600	55,900	86,600	24.7	58.6
Baseline ↓	Weld Metal ↓	Room	66,900	81,500	28.7	73.2
		Room	67,350	82,250	25.0	65.3
		300	59,700	74,600	24.0	72.9
		300	59,800	74,500	23.3	71.8
		600	57,200	79,400	23.4	65.2
		600	56,300	78,500	23.6	63.4
Capsule T ↓	W-9 W-10	Room	86,100	103,400	23.6	65.0
		550	75,800	95,300	19.3	60.8

The tensile properties of the weld metal appeared to be the most affected by the radiation exposure in Capsule T as expected from the reported copper contents.





## V. ANALYSIS OF RESULTS

The analysis of data obtained from surveillance program specimens has the following goals:

(1) Estimate the period of time over which the properties of the vessel beltline materials will meet the fracture toughness requirements of Appendix G of 10CFR50. This requires a projection of the measured reduction in  $C_v$  upper shelf energy to the vessel wall using knowledge of the energy and spatial distribution of the neutron flux and the dependence of  $C_v$  upper shelf energy on the neutron fluence.

(2) Develop heatup and cooldown curves to describe the operational limitations for selected periods of time. This requires a projection of the measured shift in  $RT_{NDT}$  to the vessel wall using knowledge of the dependence of the shift in  $RT_{NDT}$  on the neutron fluence and the energy and spatial distribution of the neutron flux.

The energy and spatial distribution of the neutron flux for Donald C. Cook Unit No. 1 was calculated for Capsule T with the DOT 3.5 discrete ordinates transport code. The lead factor for Capsule T reported by Westinghouse is 2.6 for the vessel I.D. surface.<sup>(13)</sup> This was supported by the SwRI DOT 3.5 analysis. The DOT 3.5 analysis also predicted that the fast flux at the 1/4T and 3/4T positions in the 8-5/8-in. pressure vessel wall would be 49% and 7.8%, respectively, of that at the vessel I.D. These figures are in good agreement with fluence attenuation determinations of 46% and 10% for an 8-in. steel plate by the Naval Research Laboratory.<sup>(15)</sup> However, currently the NRC prefers to use more conservative figures of 60% and 15%, respectively, for the attenuation of fast neutron flux at the 1/4T and 3/4T positions in an 8-in.

vessel wall.<sup>(16)</sup> This conservatism allows for the increased fraction of neutrons which might accrue in the 0.1 to 1.0 MeV range in deep penetration situations. For the 8-5/8-in. wall thickness of the D.C. Cook Unit No. 1 vessel, the attenuations become 57% and 12.5% for the 1/4T and 3/4T positions, respectively.

A method for estimating the reduction in  $C_v$  upper shelf energy as a function of neutron fluence is given in Regulatory Guide 1.99, Revision 1.<sup>(7)</sup> The results from Capsule T are compared to a portion of Figure 2 of Regulatory Guide 1.99, Revision 1, in Figure 9. The embrittlement response of the weld metal, reported to contain 0.27% Cu<sup>(13)</sup>, is in good agreement with the prediction of Regulatory Guide 1.99, Revision 1. However, the plate is less sensitive and the HAZ is more sensitive than predicted for the 0.14% copper content. The behavior of the HAZ specimens may reflect some copper pickup in the HAZ from the weld deposit or the placement of the notch unusually close to the fusion line. Using the dashed curve drawn through the data point for the weld metal, it is predicted that the weld metal  $C_v$  shelf energy will reach 50 ft-lbs at a fluence of about  $2.1 \times 10^{19}$  ( $E > 1$  MeV). This corresponds to approximately 38 effective full power years (EFPY) of operation at the vessel I.D., in excess of the 32 EFPY design life of the plant. The plate and HAZ materials are projected to require even larger fluences to reach the 50 ft-lb shelf level. These projections will be reexamined after the next surveillance capsule has been removed.

A similar approach can be taken to estimate the increase in  $RT_{NDT}$  as a function of reactor power generation. Figure 10 compares the Donald C. Cook Unit No. 1 surveillance data on the three surveillance materials to selected portions of Figure 1 of Regulatory Guide 1.99, Revision 1. The results

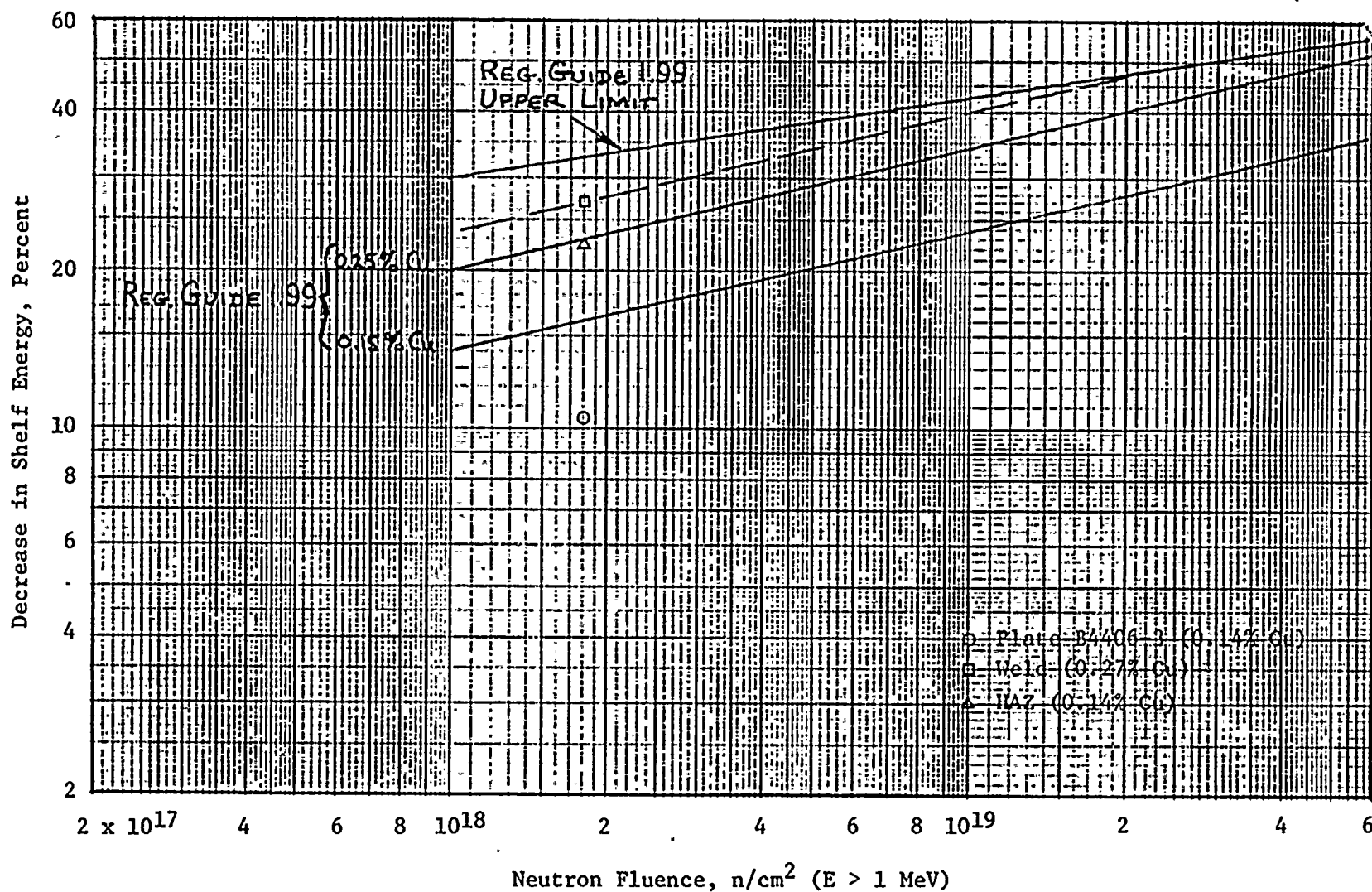


FIGURE 9. DEPENDENCE OF  $C_v$  SHELF ENERGY ON NEUTRON FLUENCE, DONALD C. COOK UNIT NO. 1

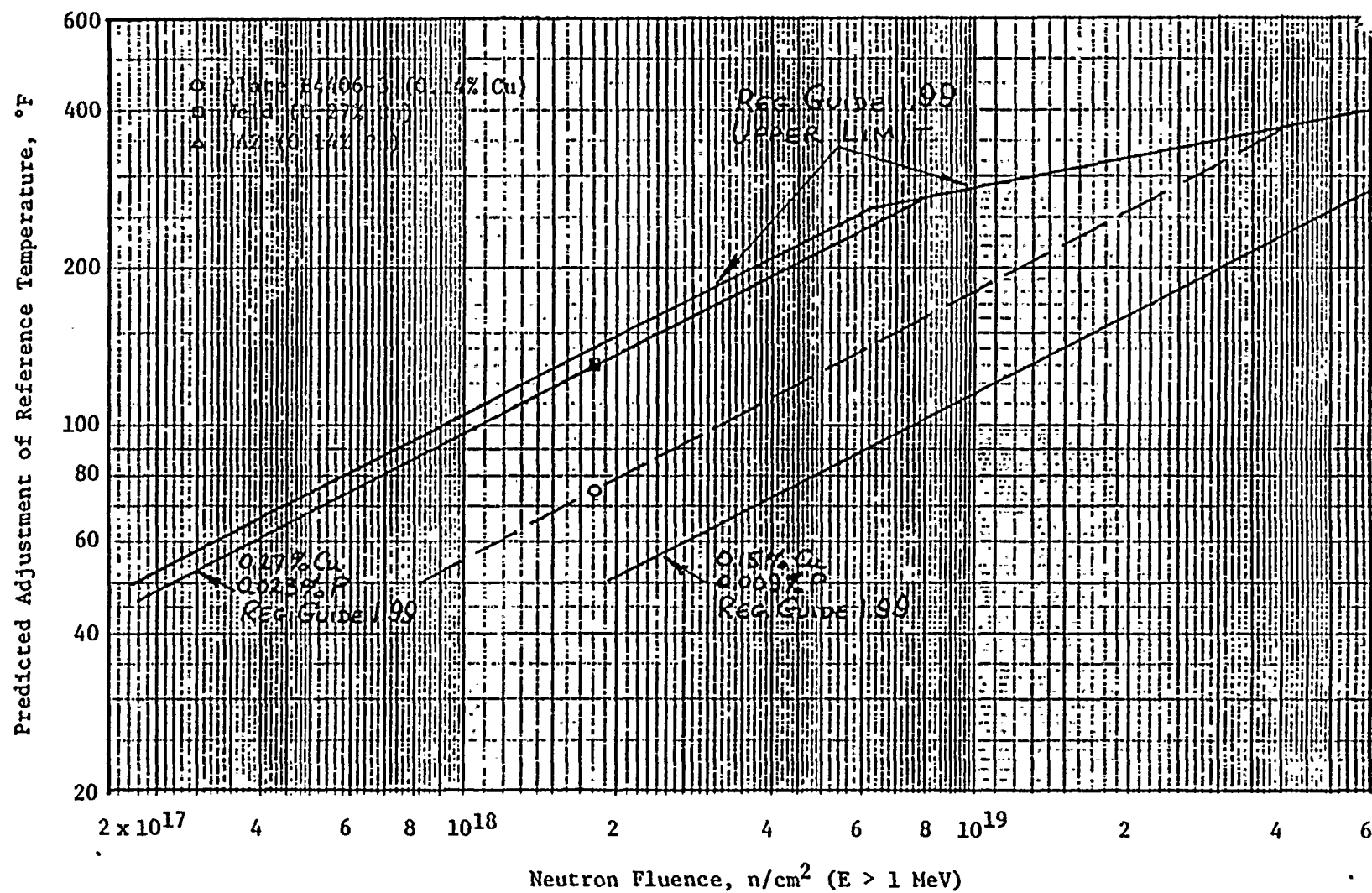


FIGURE 10. EFFECT OF NEUTRON FLUENCE ON  $RT_{NDT}$  SHIFT, DONALD C. COOK UNIT NO. 1

indicate that the measured shift in  $RT_{NDT}$  of the weld metal is in agreement with that predicted by Regulatory Guide 1.99, Revision 1, but that the measured shifts in  $RT_{NDT}$  for the plate and HAZ materials are underpredicted by the guide.

The predicted shifts in  $RT_{NDT}$  for the Donald C. Cook Unit No. 1 reactor pressure vessel obtained from Figure 10 are summarized in Tables XII and XIII. The values predicted at the 1/4T and 3/4T after 12 EFPY (Table XII) are used to develop heatup and cooldown limit curves to meet the requirements of Appendix G to Section III of the ASME Code, as described in Section VI of this report. These projections for  $C_v$  shelf energy reductions and  $RT_{NDT}$  shifts, and the resulting heatup and cooldown limit curves, are based on extrapolations from one data point representing the most sensitive material. After a second capsule has been removed and tested, one will be able to interpolate between two data points.

The Donald C. Cook Unit No. 1 reactor vessel surveillance program schedule proposed by Westinghouse<sup>(13)</sup> is summarized in Table XIV. It has been organized to satisfy Appendix H of 10CFR50 as closely as possible. There are seven additional capsules in the vessel, all of which contain base plate, weld metal and HAZ specimens. There is no reason to consider changing the proposed capsule removal schedule at this time.

TABLE XII

PROJECTED VALUES OF  $RT_{NDT}$  FOR DONALD C. COOK UNIT NO. 1 FOR UP TO 12 EFPY OF OPERATION

Location	Material	Calculated Fluence ( $n/cm^2$ , $E > 1$ MeV)	$RT_{NDT}$ (deg F)		
			Initial	Shift	12 EFPY <sup>(a)</sup>
Vessel I.D. ↓	Inter. Shell Plate	$6.55 \times 10^{18}$	45(b)	145	190
	Weld Metal	↓	-52(b)	245	193
	HAZ	↓	-60(c)	245	185
Vessel 1/4T ↓	Inter. Shell Plate	$3.73 \times 10^{18}$	45(b)	110	155
	Weld Metal	↓	-52(b)	185	133
	HAZ	↓	-60(c)	185	125
Vessel 3/4T ↓	Inter. Shell Plate	$8.2 \times 10^{17}$	45(b)	50	95
	Weld Metal	↓	-52(b)	87	35
	HAZ	↓	-60(c)	87	27

(a) 1 EFPY = 1,186,250  $MWD_t$ .

(b) Reference 18.

(c) References 13 and 18.

TABLE XIII

PROJECTED VALUES OF  $RT_{NDT}$  FOR DONALD C. COOK UNIT NO. 1 FOR UP TO 32 EFPY OF OPERATION

Location	Material	Calculated Fluence ( $n/cm^2$ , $E > 1$ MeV)	$RT_{NDT}$ (deg F)		
			Initial	Shift	32 EFPY (a)
Vessel I.D. ↓	Inter. Shell Plate	$1.75 \times 10^{19}$	45(b)	240	285
	Weld Metal	↓	-52(b)	320	268
	HAZ	↓	-60(c)	320	260
Vessel 1/4T ↓	Inter. Shell Plate	$1.0 \times 10^{19}$	45(b)	180	225
	Weld Metal	↓	-52(b)	285	233
	HAZ	↓	-60(c)	285	225
Vessel 3/4T ↓	Inter. Shell Plate	$2.2 \times 10^{18}$	45(b)	83	128
	Weld Metal	↓	-52(b)	142	90
	HAZ	↓	-60(c)	142	82

(a) 1 EFPY = 1,186,250  $MWD_t$ .

(b) Reference 18.

(c) References 13 and 18.



TABLE XIV

PROPOSED REACTOR VESSEL SURVEILLANCE CAPSULE SCHEDULE  
DONALD C. COOK UNIT NO. 1

<u>Capsule Identification</u>	<u>Lead Factor</u>	<u>Removal Time</u>
T	2.6	Removed and tested at end of first core cycle
X	2.6	10 Years (postirradiation test)
S	0.6	10 Years (reinsert in Capsule T location)
V	0.6	10 Years (reinsert in Capsule X location)
U	2.6	20 Years (postirradiation test)
W	0.6	20 Years (reinsert in Capsule U location)
Y	2.6	30 Years (postirradiation test)
Z	0.6	30 Years (reinsert in Capsule Y location)

## VI. HEATUP AND COOLDOWN LIMIT CURVES FOR NORMAL OPERATION OF DONALD C. COOK UNIT NO. 1

Donald C. Cook Unit No. 1 is a 3250 Mw<sub>t</sub> pressurized water reactor operated by American Electric Power Service Corporation. The unit has been provided with a reactor vessel material surveillance program as required by 10CFR50, Appendix H.

The first surveillance capsule (Capsule T) was removed during the 1977 refuelling outage. This capsule was tested by Southwest Research Institute, the results being described in the earlier sections of this report. In summary, these results indicate that:

(1) The RT<sub>NDT</sub> of the surveillance materials in Capsule T increased a maximum of 130 F as a result of exposure to a neutron fluence of  $1.80 \times 10^{18}$  neutrons/cm<sup>2</sup> (E > 1 MeV).

(2) Based on a ratio of 2.6 between the fast neutron flux at the Capsule T location and the maximum incident on the vessel wall, the vessel wall fluence at the I.D. was  $6.92 \times 10^{17}$  neutrons/cm<sup>2</sup> (E > 1 MeV) at the time of removal of Capsule T.

(3) The maximum shift in RT<sub>NDT</sub> after 12 effective full power years (EFPY) of operation was predicted to be 185 F at the 1/4T and 87 F at the 3/4T vessel wall locations, as controlled by the weld metal and HAZ materials.

(4) The intermediate shell plate material, although less sensitive to radiation embrittlement than the weld and HAZ materials, is projected to control the limiting RT<sub>NDT</sub> for a considerable length of time because of a much higher initial (unirradiated) RT<sub>NDT</sub> of 45 F. (18)

The Unit No. 1 heatup and cooldown limit curves for 12 EFPY have been computed on the basis of (4) above because it is anticipated that the  $RT_{NDT}$  of the primary pressure boundary materials will be highest for the plate material at least through that time period (see Table XII). The procedures employed by SwRI are described in Appendix B.

The following pressure vessel constants were employed as input data in this analysis:

Vessel Inner Radius, $r_i$	=	86.50 in., including cladding
Vessel Outer Radius, $r_o$	=	95.34 in.
Operating Pressure, $P_o$	=	2235 psig
Initial Temperature, $T_o$	=	70°F
Final Temperature, $T_f$	=	550°F
Effective Coolant Flow Rate, $Q$	=	$135.6 \times 10^6$ lb <sub>m</sub> /hr
Effective Flow Area, $A$	=	26.72 ft <sup>2</sup>
Effective Hydraulic Diameter, $D$	=	15.05 in.

Heatup curves were computed for a heatup rate of 60 F/hr. Since lower rates tend to raise the curve in the central region (see Appendix B), these curves apply to all heating rates up to 60 F/hr. Cooldown curves were computed for cooldown rates of 0 F/hr (steady state), 20 F/hr, 40 F/hr, 60 F/hr, and 100 F/hr. The 20 F/hr curve would apply to cooldown rates up to 20 F/hr; the 40 F/hr curve would apply to rates from 20 F to 40 F/hr; the 60 F/hr curve would apply to rates from 40 F to 60 F/hr; the 100 F/hr curve would apply to rates from 60 F/hr to 100 F/hr.

The Unit No. 1 heatup and cooldown curves for up to 12 EFPY are given in Figures 11 and 12.

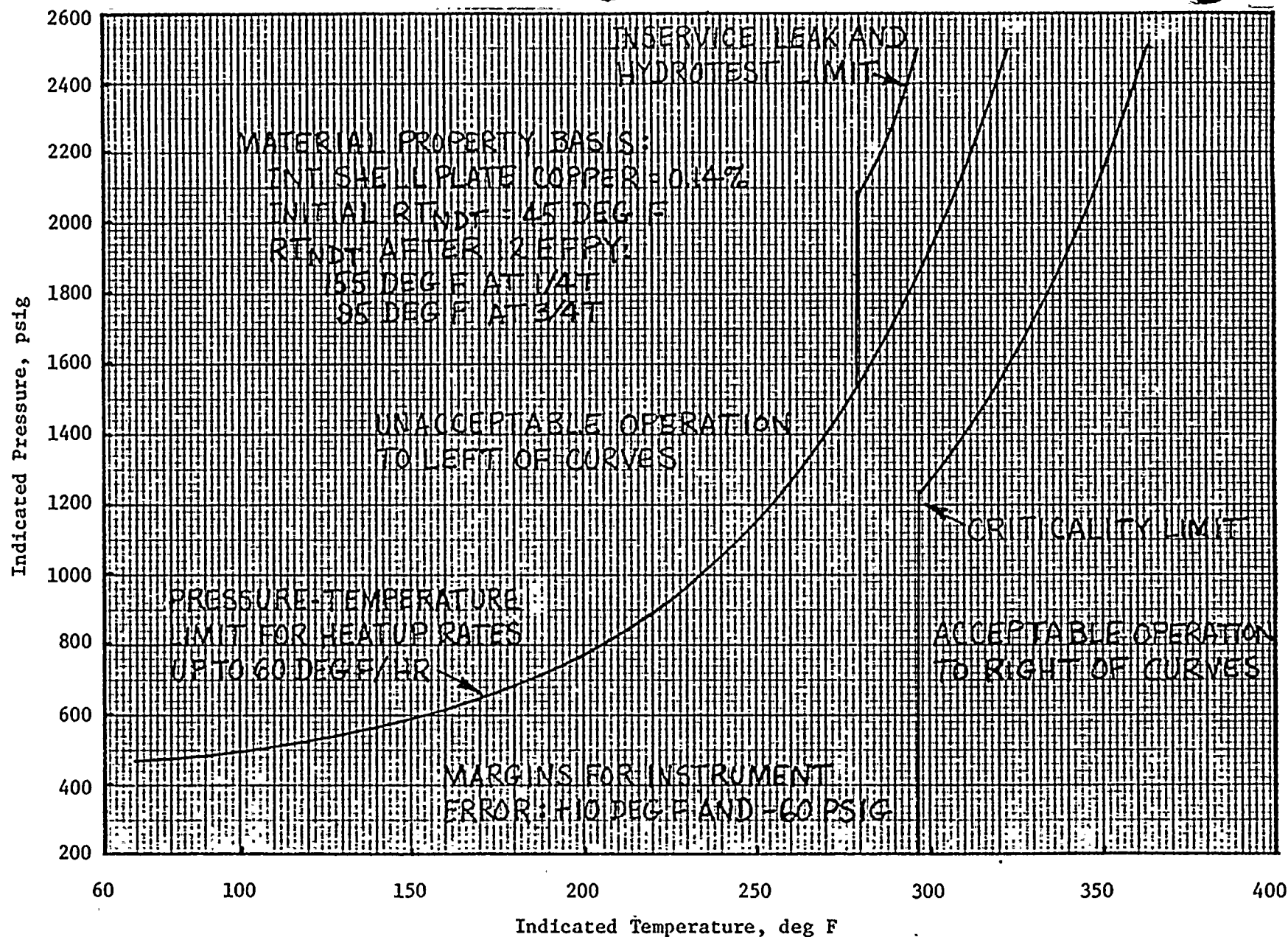


FIGURE 11. DONALD C. COOK UNIT NO. 1 REACTOR COOLANT HEATUP LIMITATIONS APPLICABLE FOR PERIODS UP TO 12 EFFECTIVE FULL POWER YEARS

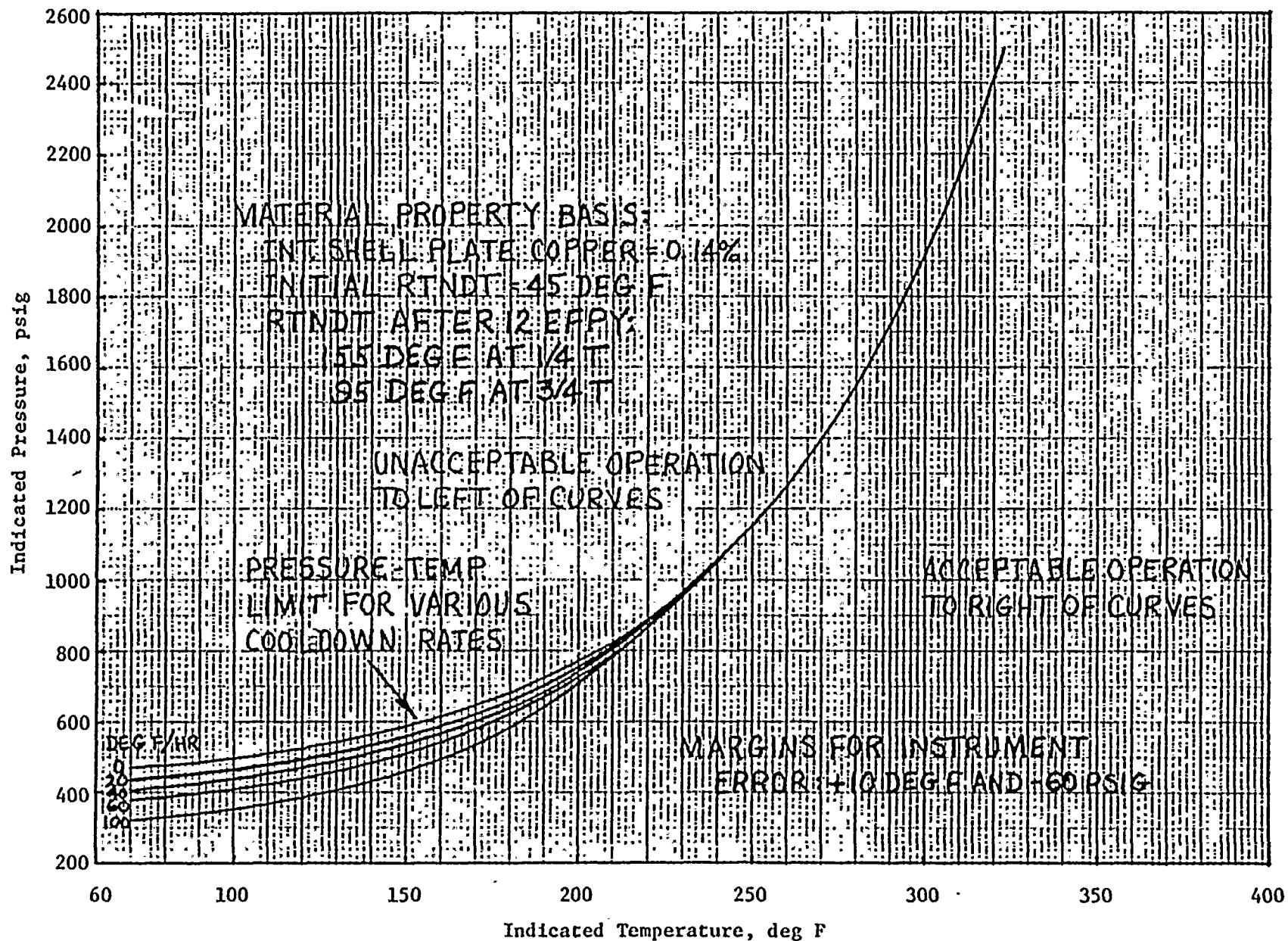


FIGURE 12. DONALD C. COOK UNIT NO. 1 REACTOR COOLANT COOLDOWN LIMITATIONS APPLICABLE FOR PERIODS UP TO 12 EFFECTIVE FULL POWER YEARS

## VII. REFERENCES

1. Title 10, Code of Federal Regulations, Part 50, "Licensing of Production and Utilization Facilities."
2. ASME Boiler and Pressure Vessel Code, Section III, "Nuclear Power Plant Components," 1974 Edition.
3. ASTM E 208-69, "Standard Method for Conducting Drop-Weight Test to Determine Nil-Ductility Transition Temperature of Ferritic Steels," 1975 Annual Book of ASTM Standards.
4. Steele, L. E., and Serpan, C. Z., Jr., "Analysis of Reactor Vessel Radiation Effects Surveillance Programs," ASTM STP 481, December 1970.
5. Steele, L. E., "Neutron Irradiation Embrittlement of Reactor Pressure Vessel Steels," International Atomic Energy Agency, Technical Reports Series No. 163, 1975.
6. ASME Boiler and Pressure Vessel Code, Section XI, "Rules for Inservice Inspection of Nuclear Power Plant Components," 1974 Edition.
7. Regulatory Guide 1.99, Revision 1, Office of Standards Development, U.S. Nuclear Regulatory Commission, April 1977.
8. Comments on Regulatory Guide 1.99, Westinghouse Electric Corporation, Obtained from NRC Public Document Room, Washington, D.C.
9. Position on Regulatory Guide 1.99, Combustion Engineering Power Systems, Obtained from NRC Public Document Room, Washington, D.C.
10. ASTM E 185-73, "Standard Recommended Practice for Surveillance Tests for Nuclear Reactor Vessels," 1975 Annual Book of ASTM Standards.
11. ASTM E 399-74, "Standard Method of Test for Plane-Strain Fracture Toughness of Metallic Materials," 1975 Annual Book of ASTM Standards.
12. Witt, F. J., and Mager, T. R., "A Procedure for Determining Bounding Values of Fracture Toughness  $K_{IC}$  at Any Temperature," ORNL-TM-3894, October 1972.
13. "American Electric Power Service Corporation Donald C. Cook Unit No. 1 Reactor Vessel Radiation Surveillance Program," WCAP-8047, March 1973.
14. ENDF/B-IV, Dosimetry Tape 412, Mat No. 6417 (26-Fe-54), July 1974.
15. Loss, F. J., Hawthorne, J. R., Serpan, C. Z., Jr., and Puzak, P. P., "Analysis of Radiation-Induced Embrittlement Gradients on Fracture Characteristics of Thick-Walled Pressure Vessel Steels," NRL Report 7209, March 1, 1971.

16. Telecon, E. B. Norris to Ken Hogue (NRC Staff) January 19, 1977.
17. Hazleton, W. S., Anderson, S. L., and Yanichko, S. E., "Basis for Heatup and Cooldown Limit Curves," WCAP-7924, July 1972.
18. Donald C. Cook Unit No. 1 Technical Specifications, as of November 30, 1977.

APPENDIX A

TENSILE TEST RECORDS



Southwest Research Institute  
Department of Materials Sciences  
TENSILE TEST DATA SHEET

Test No. T- 1 Est. U. T. S. \_\_\_\_\_ psi Project No. 02-4770-001  
Spec. No. A-1 Initial G. L. 1.000 in. Machine No. D1LL02  
Temperature 84 °F Initial Dia. .249 in. Date 7/3.5/77  
Strain Rate .02 "/min Initial Thickness \_\_\_\_\_ in. Initial Area .0487  
Initial Width \_\_\_\_\_ in. (60)

Top Temperature \_\_\_\_\_ °F Maximum Load 4860 lb  
Bottom Temperature \_\_\_\_\_ °F 0.2% Offset Load 3540 lb  
Final Gage Length 1.243 in. 0.02% Offset Load \_\_\_\_\_ lb  
Final Diameter .146 in. Upper Yield Point \_\_\_\_\_ lb  
Final Area .0167 in.<sup>2</sup>  
(60)

$$\text{U. T. S.} = \frac{\text{Maximum Load}}{\text{Initial Area}} = \frac{4860}{.0487} \text{ psi} = 99792 \text{ psi}$$

$$0.2\% \text{ Y. S.} = \frac{0.2\% \text{ Offset Load}}{\text{Initial Area}} = \frac{3540}{.0487} \text{ psi} = 72690 \text{ psi}$$

$$0.02\% \text{ Y. S.} = \frac{0.02\% \text{ Offset Load}}{\text{Initial Area}} = \text{_____} \text{ psi}$$

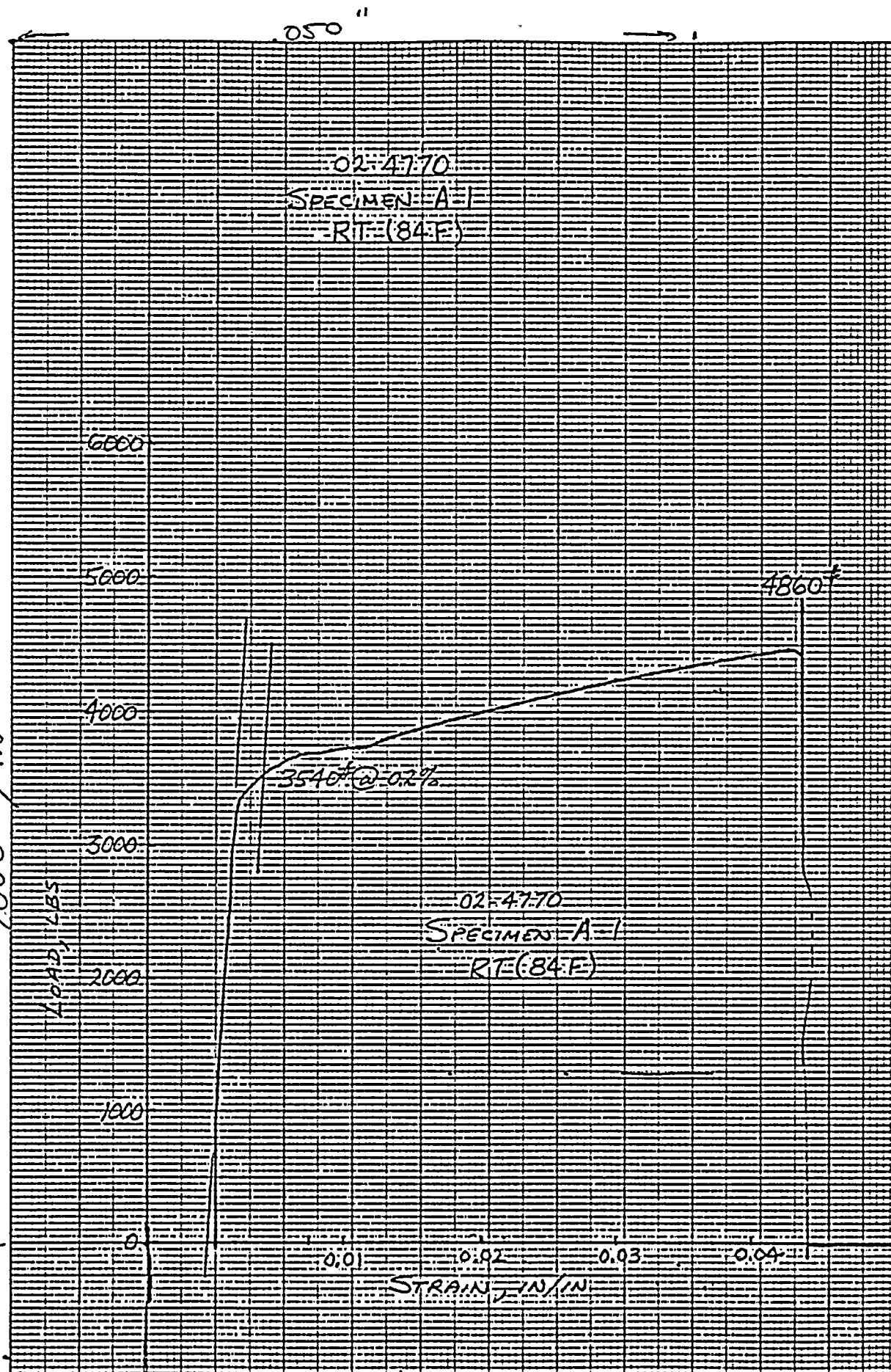
$$\text{Upper Y. S.} = \frac{\text{Upper Yield Point}}{\text{Initial Area}} = \text{_____} \text{ psi}$$

$$\% \text{ Elongation} = \frac{\text{Final G. L.} - \text{Initial G. L.}}{\text{Initial G. L.}} \times 100 = \frac{1.243 - 1.000}{1.000} \times 100 = 24.3 \%$$

$$\% \text{ R. A.} = \frac{\text{Initial Area} - \text{Final Area}}{\text{Initial Area}} \times 100 = \frac{.0487 - .0167}{.0487} \times 100 = 65.7 \%$$
(61)

Signature: [Signature]

checked  
E.B.  
8/5/77



A-3

.01"/in and @

Southwest Research Institute  
Department of Materials Sciences  
TENSILE TEST DATA SHEET

Test No. T- 2 Est. U. T. S. \_\_\_\_\_ psi Project No. 02-4770-001  
Spec. No. W-9 Initial G. L. 1.0 in. Machine No. DILLON  
Temperature 84 °F Initial Dia. .250 in. Date 7-25-77  
Strain Rate .02"/min Initial Thickness \_\_\_\_\_ in. Initial Area .0491  
Initial Width \_\_\_\_\_ in. *CP*

Top Temperature \_\_\_\_\_ °F Maximum Load 5075 lb  
Bottom Temperature \_\_\_\_\_ °F 0.2% Offset Load 4250 lb  
Final Gage Length 1.236 in. 0.02% Offset Load \_\_\_\_\_ lb  
Final Diameter .148 in. Upper Yield Point \_\_\_\_\_ lb  
Final Area .0172 ✓ in.<sup>2</sup>

$$\text{U. T. S.} = \frac{\text{Maximum Load}}{\text{Initial Area}} = \frac{103,400}{\text{CP}} \text{ psi}$$

$$0.2\% \text{ Y. S.} = \frac{0.2\% \text{ Offset Load}}{\text{Initial Area}} = \frac{86,150}{\text{CP}} \text{ psi}$$

$$0.02\% \text{ Y. S.} = \frac{0.02\% \text{ Offset Load}}{\text{Initial Area}} = \text{_____} \text{ psi}$$

$$\text{Upper Y. S.} = \frac{\text{Upper Yield Point}}{\text{Initial Area}} = \text{_____} \text{ psi}$$

$$\% \text{ Elongation} = \frac{\text{Final G. L.} - \text{Initial G. L.}}{\text{Initial G. L.}} \times 100 = \frac{23.6}{\text{CP}} \%$$

$$\% \text{ R. A.} = \frac{\text{Initial Area} - \text{Final Area}}{\text{Initial Area}} \times 100 = \frac{65.0}{\text{CP}} \%$$

Signature: *Richard D. Smith*

02-4770  
SPECIMEN W-9  
RT (84°F)

6000

5000

4000

3000

2000

1000

5075

4230# @ 0.2%

02-4770  
SPECIMEN W-9  
RT (84°F)

A-5

1070 / IN.

Southwest Research Institute  
Department of Materials Sciences

TENSILE TEST DATA SHEET

Test No. T- 3 Est. U. T. S. \_\_\_\_\_ psi Project No. 02-4770.001  
Spec. No. A2 Initial G. L. 1.000 in. Machine No. 11101  
Temperature 550 °F Initial Dia. .149 in. Date 7/16/77  
Strain Rate .02 in/in Initial Thickness \_\_\_\_\_ in. Initial Area .0487  
Initial Width \_\_\_\_\_ in. (20)

Top Temperature 551 °F Maximum Load 4530 lb  
Bottom Temperature 548 °F 0.2% Offset Load 3250 lb  
Final Gage Length 1.202 in. 0.02% Offset Load \_\_\_\_\_ lb  
Final Diameter .149 in. Upper Yield Point \_\_\_\_\_ lb  
Final Area .0174 in.<sup>2</sup> ✓

U. T. S. =  $\frac{\text{Maximum Load}}{\text{Initial Area}}$  = 93,020 psi (21)

0.2% Y. S. =  $\frac{0.2\% \text{ Offset Load}}{\text{Initial Area}}$  = 66,740 psi (22)

0.02% Y. S. =  $\frac{0.02\% \text{ Offset Load}}{\text{Initial Area}}$  = \_\_\_\_\_ psi

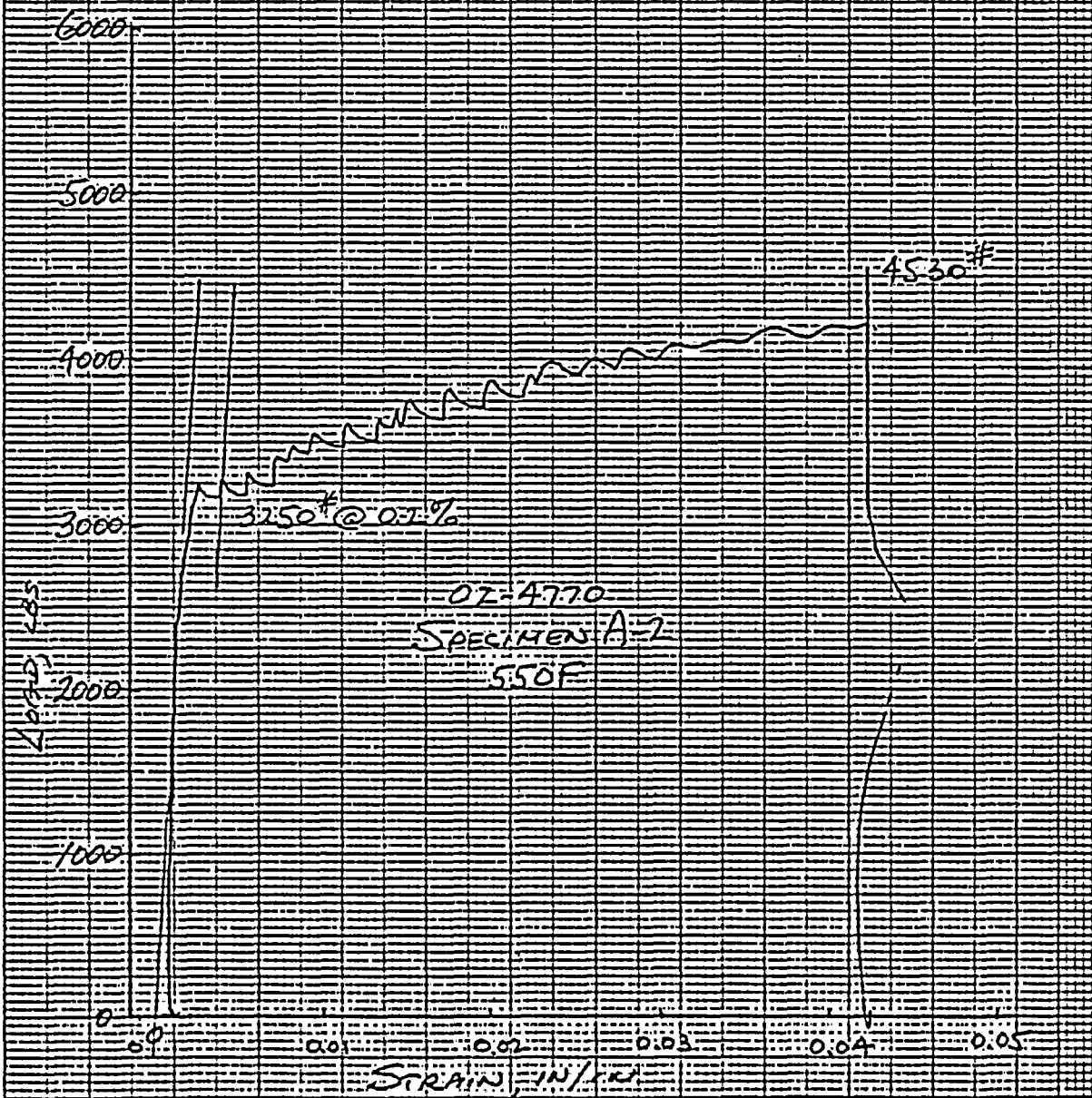
Upper Y. S. =  $\frac{\text{Upper Yield Point}}{\text{Initial Area}}$  = \_\_\_\_\_ psi

% Elongation =  $\frac{\text{Final G. L.} - \text{Initial G. L.}}{\text{Initial G. L.}} \times 100$  = 20.2 % ✓

% R. A. =  $\frac{\text{Initial Area} - \text{Final Area}}{\text{Initial Area}} \times 100$  = 64.3 % (23)

Signature: Robert L. Holt

02-4770  
SPECIMEN A-1  
550F



02-4770  
SPECIMEN A-2  
550F

Southwest Research Institute  
Department of Materials Sciences  
TENSILE TEST DATA SHEET

Test No. T- A Est. U.T.S. \_\_\_\_\_ psi Project No. 62-1720-001  
Spec. No. W10 Initial G. L. 1.000 in. Machine No. D11122  
Temperature 550 °F Initial Dia. .249 in. Date 7/56/77  
Strain Rate .02 in/in Initial Thickness \_\_\_\_\_ in. Initial Area .0487  
Initial Width \_\_\_\_\_ in. CVI

Top Temperature 548 °F Maximum Load 4640 lb  
Bottom Temperature 546 °F 0.2% Offset Load 3690 lb  
Final Gage Length 1.193 in. 0.02% Offset Load \_\_\_\_\_ lb  
Final Diameter .156 in. Upper Yield Point \_\_\_\_\_ lb  
Final Area .0191 in.<sup>2</sup>

$$\text{U. T. S.} = \frac{\text{Maximum Load}}{\text{Initial Area}} = \frac{75,280}{.0487} \text{ psi}$$

$$0.2\% \text{ Y. S.} = \frac{0.2\% \text{ Offset Load}}{\text{Initial Area}} = \frac{75,770}{.0487} \text{ psi}$$

$$0.02\% \text{ Y. S.} = \frac{0.02\% \text{ Offset Load}}{\text{Initial Area}} = \text{_____} \text{ psi}$$

$$\text{Upper Y. S.} = \frac{\text{Upper Yield Point}}{\text{Initial Area}} = \text{_____} \text{ psi}$$

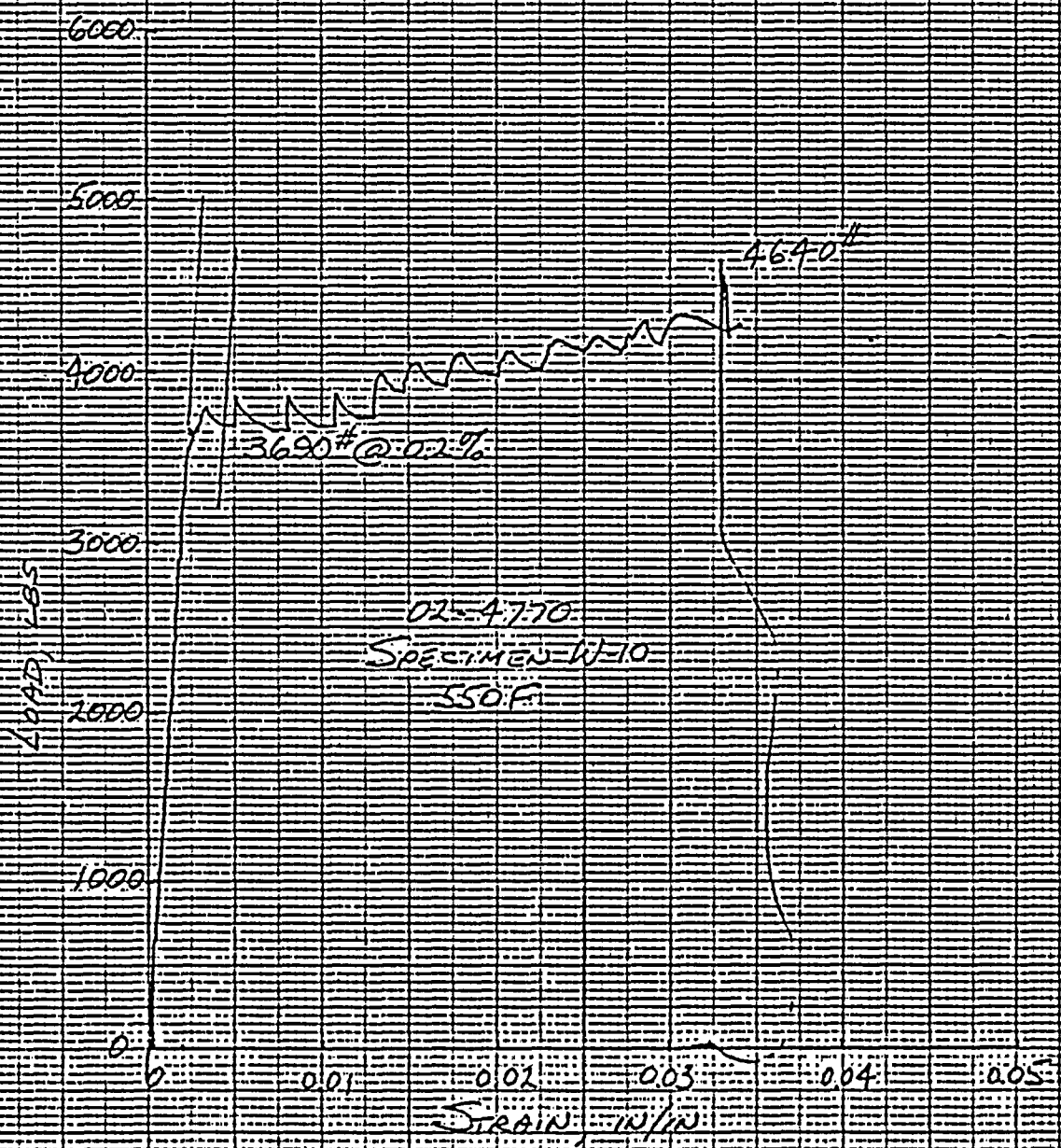
$$\% \text{ Elongation} = \frac{\text{Final G. L.} - \text{Initial G. L.}}{\text{Initial G. L.}} \times 100 = \frac{19.3}{1.000} \%$$

$$\% \text{ R. A.} = \frac{\text{Initial Area} - \text{Final Area}}{\text{Initial Area}} \times 100 = \frac{.0296}{.0487} \%$$

Signature: R. L. S. [Signature]

Checked  
[Signature]  
6/5/77

02-4770  
SPECIMEN W-10  
550-F







APPENDIX B

PROCEDURE FOR THE GENERATION OF ALLOWABLE  
PRESSURE-TEMPERATURE LIMIT CURVES FOR  
NUCLEAR POWER PLANT REACTOR VESSELS

PROCEDURE FOR THE GENERATION OF ALLOWABLE  
PRESSURE-TEMPERATURE LIMIT CURVES FOR  
NUCLEAR POWER PLANT REACTOR VESSELS

A.     Introduction

The following is a description of the basis for the generation of pressure-temperature limit curves for inservice leak and hydrostatic tests, heatup and cooldown operations, and core operation of reactor pressure vessels. The safety margins employed in these procedures equal or exceed those recommended in the ASME Boiler and Pressure Vessel Code, Section III, Appendix G, "Protection Against Nonductile Failure."

B.     Background

The basic parameter used to determine safe vessel operational conditions is the stress intensity factor,  $K_I$ , which is a function of the stress state and flaw configuration. The  $K_I$  corresponding to membrane tension is given by

$$K_{Im} = M_m \cdot \sigma_m \quad (1)$$

where  $M_m$  is the membrane stress correction factor for the postulated flaw and  $\sigma_m$  the membrane stress. Likewise,  $K_I$  corresponding to bending is given by

$$K_{Ib} = M_b \cdot \sigma_b \quad (2)$$

where  $M_b$  is the bending stress correction factor and  $\sigma_b$  is the bending stress. For vessel section thickness of 4 to 12 inches, the maximum

postulated surface flaw, which is assumed to be normal to the direction of maximum stress, has a depth of 0.25 of the section thickness and a length of 1.50 times the section thickness. Curves for  $M_m$  versus the square root of the vessel wall thickness for the postulated flaw are given in Figure 1 as taken from the Pressure Vessel Code (ref. Figure G-2114.1). These curves are a function of the stress ratio parameter  $\sigma/\sigma_y$ , where  $\sigma_y$  is the material yield strength which is taken to be 50,000 psi. The bending correction factor is defined as  $2/3 M_m$  and is therefore determined from Figure 1 as well. The basis for these curves is given in ASME Boiler and Pressure Vessel Code, Section XI, "Rules for Inservice Inspection of Nuclear Power Plant Components," Article A-3000.

The Code specifies the minimum  $K_I$  that can cause failure as a function of material temperature,  $T$ , and its reference nil ductility temperature,  $RT_{NDT}$ . This minimum  $K_I$  is defined as the reference stress intensity factor,  $K_{IR}$ , and is given by

$$K_{IR} = 26777. + 1223. \exp \left[ 0.014493(T - RT_{NDT} + 160) \right] \quad (3)$$

where all temperatures are in degrees Fahrenheit. A plot of this expression is given in Figure 2 taken from the Code (ref. Figure G-2010.1).

### C. Pressure-Temperature Relationships

#### 1. Inservice Leak and Hydrostatic Test

During performance of inservice leak and hydrostatic tests, the reference stress intensity factor,  $K_{IR}$ , must always be greater than

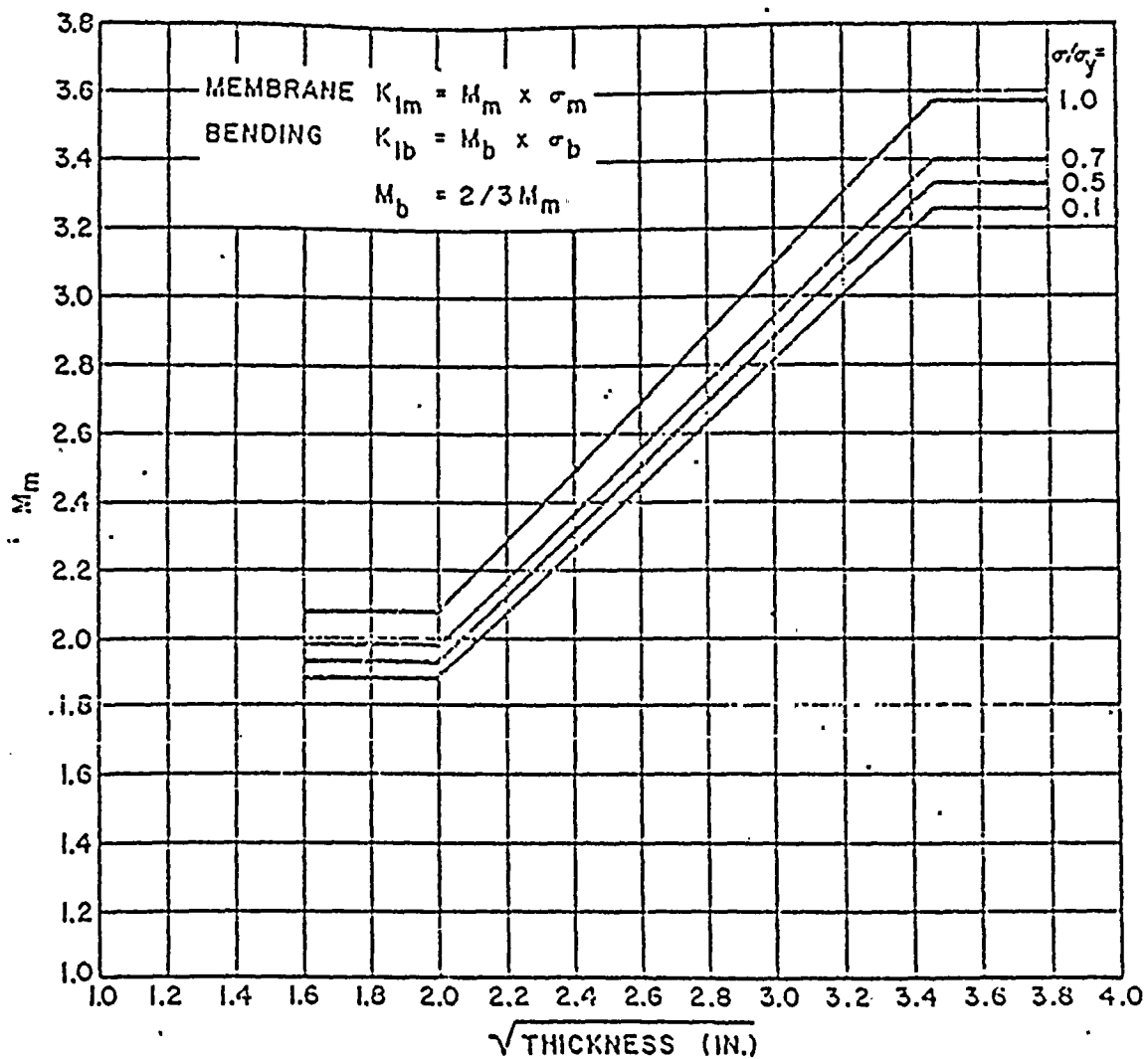


FIGURE 1. STRESS CORRECTION FACTOR

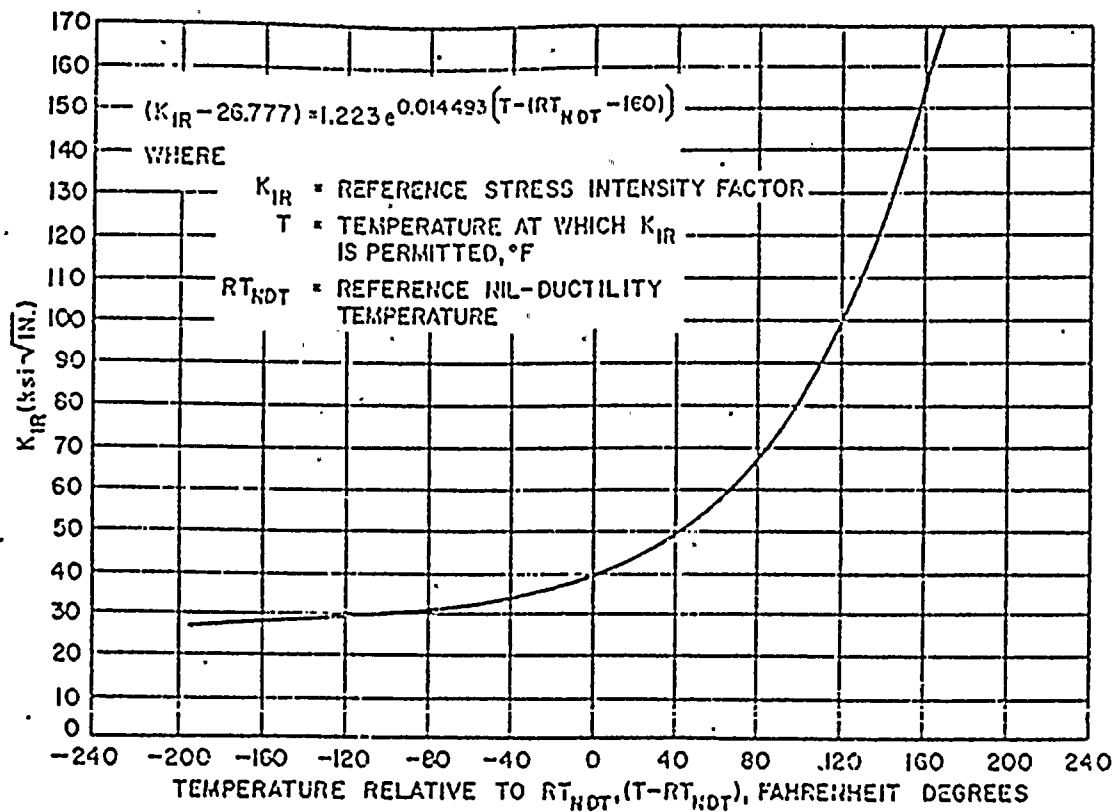


FIGURE 2. REFERENCE STRESS INTENSITY FACTOR

1.5 times the  $K_I$  caused by pressure, thus

$$1.5 K_{Ip} < K_{IR} \quad (4)$$

or

$$1.5 M_m \sigma_m < K_{IR} \quad (5)$$

For a cylinder with inner radius  $r_i$  and outer radius  $r_o$ , the stress distribution due to internal pressure is given by

$$\sigma(r) = \left( \frac{r_i^2}{r_o^2 - r_i^2} \right) \left( \frac{r_o^2 + r^2}{r^2} \right) \quad (6)$$

With 1/4T flaws possible at both inner and outer radial locations, i.e., at  $r_{1/4} = r_i + 1/4(r_o - r_i)$  and  $r_{3/4} = r_i + 3/4(r_o - r_i)$ , the maximum stress will occur at the inner flaw location, thus

$$\sigma_{\max} = P_o \left( \frac{r_i^2}{r_o^2 - r_i^2} \right) \left[ \frac{r_o^2 + (1/4r_o + 3/4r_i)^2}{(1/4r_o + 3/4r_i)^2} \right] \quad (7)$$

With the operation pressure known, i.e.,  $P_o$ , we determine the minimum coolant temperature that will satisfy Equation (4) by evaluating

$$K_{IR} = 1.5 M_m \sigma_{\max} \quad (8)$$

and determine the corresponding coolant temperature,  $T$ , from Equation (3) for the given  $RT_{NDT}$  at the 1/4T location. For this calculation, Equation (3) takes the form

$$T = RT_{NDT}(1/4T) - 160. + 68.9988 \ln \left[ \frac{K_{IR} - 26777.}{1223.} \right] \quad (9)$$

The inservice curves are generated for an operating pressure range of  $.96 P_0$  to  $1.14 P_0$ , where  $P_0$  is the design operating pressure.

## 2. Heatup and Cooldown Operations

At all times during heatup and cooldown operations, the reference stress intensity factor,  $K_{IR}$ , must always be greater than the sum of 2 times the  $K_{IP}$  caused by pressure and the  $K_{It}$  caused by thermal gradients, thus

$$2.0 K_{IP} + 1.0 K_{It} < K_{IR} \quad (10)$$

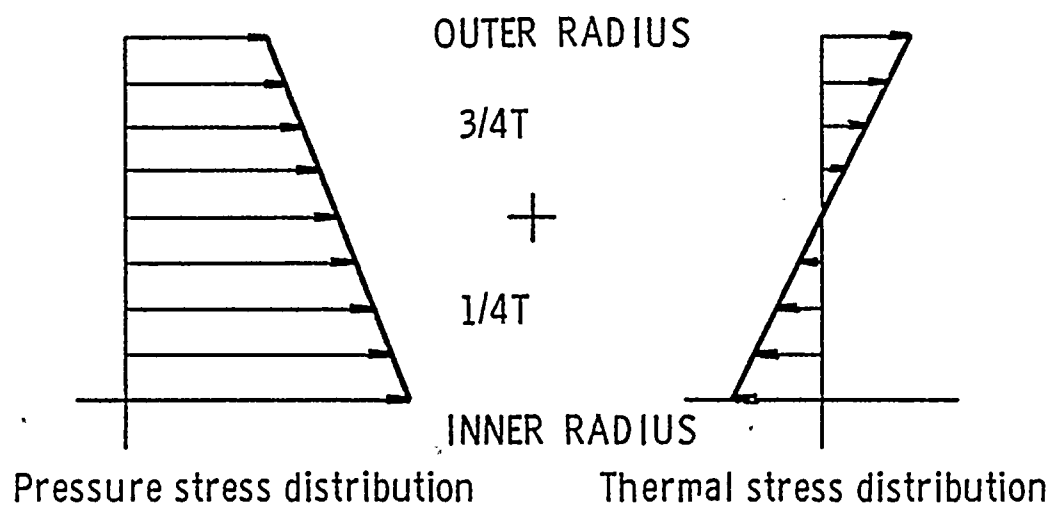
or

$$2.0 M_m \sigma_{max} = K_{IR} - K_{It} \quad (11)$$

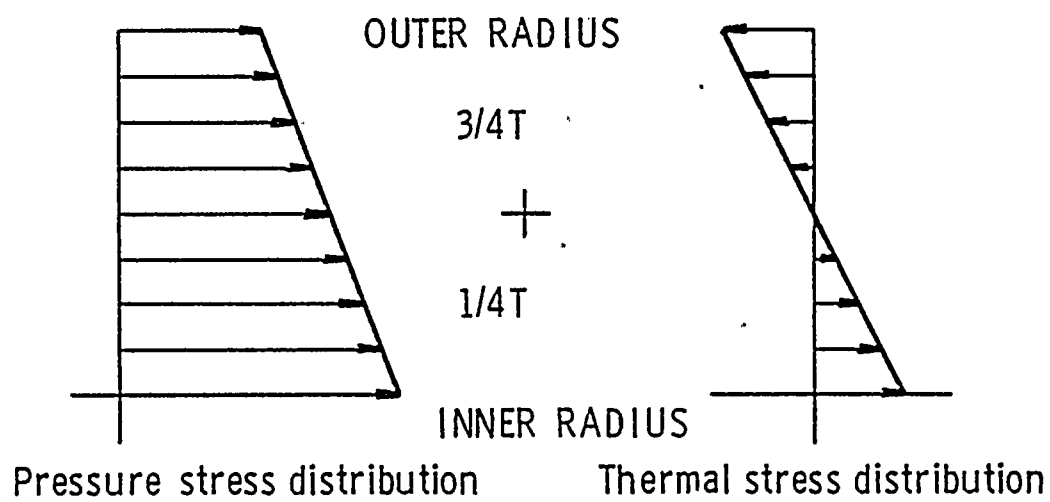
where  $\sigma_{max}$  is the maximum allowable stress due to internal pressure, and  $K_{It}$  is the equivalent linear stress intensity factor produced by the thermal gradients. To obtain the equivalent linear stress intensity factor due to thermal gradients requires a detailed thermal stress analysis. The details of the required analysis are given in Section D.

During heatup the radial stress distributions due to internal pressure and thermal gradients are shown schematically in Figure 3a. Assuming a possible flaw at the  $1/4T$  location, we see from Figure 3a that the thermal stress tends to alleviate the pressure stress at this point in the vessel wall and, therefore, the steady state pressure stress would represent the maximum stress condition at the  $1/4T$  location. At





( a ) Heatup



( b ) Cooldown

Figure 3. Heatup and Cooldown Stress Distribution

the 3/4T flaw location, the pressure stress and thermal stress add and, therefore, the combination for a given heatup rate represents the maximum stress at the 3/4T location. The maximum overall stress between the 1/4T and 3/4T location then determines the maximum allowable reactor pressure at the given coolant temperature.

The heatup pressure-temperature curves are thus generated by calculating the maximum steady state pressure based on a possible flaw at the 1/4T location from

$$P_{\max}(1/4T) = \frac{K_{IR}}{2M_m \left( \frac{r_i^2}{r_o^2 - r_i^2} \right) \left( \frac{r_o^2 + (1/4r_o + 3/4r_i)^2}{(1/4r_o + 3/4r_i)^2} \right)} \quad (12)$$

where  $M_m$  is determined from the curves in Figure 1 and  $K_{IR}$  is obtained from Equation (3) using the coolant temperature and  $RT_{NDT}$  at the 1/4T location. Here we may note that  $M_m$  must be iterated for since it is a function of the final stress ratio to yield strength ( $\sigma/\sigma_y$ ).

At the 3/4T location, the maximum pressure is determined from Equation (11) as

$$P_{\max}(3/4T) = \frac{K_{IR} - K_{It}}{2M_m \left( \frac{r_i^2}{r_o^2 - r_i^2} \right) \left( \frac{r_o^2 + (1/4r_i + 3/4r_o)^2}{(1/4r_i + 3/4r_o)^2} \right)} \quad (13)$$

where  $K_{IR}$  is obtained from Equation (2) using the material temperature and  $RT_{NDT}$  at the 3/4T location and  $K_{It}$  is determined from the analysis procedure outlined in Section D.  $M_m$  is determined from Figure 1.

The minimum of these maximum allowable pressures at the given coolant temperature determines the maximum operation pressure. Each heatup rate of interest must be analyzed on an individual basis.

The cooldown analysis proceeds in a similar fashion as that described for heatup with the following exceptions: We note from Figure 3b that during cooldown the 1/4T location always controls the maximum stress since the thermal gradient produces tensile stresses at the 1/4T location. Thus the steady state pressure is the same as that given in Equation (12). For each cooldown rate, the maximum pressure is evaluated at the 1/4T location from

$$P_{\max}(1/4T) = \frac{K_{IR} - K_{It}}{2M_m \left( \frac{r_i^2}{r_o^2 - r_i^2} \right) \left( \frac{r_o^2 + (3/4r_i + 1/4r_o)^2}{(3/4r_i + 1/4r_o)} \right)} \quad (14)$$

where  $K_{IR}$  is obtained from Equation (3) using the material temperature and  $RT_{NDT}$  at the 1/4T location.  $K_{It}$  is determined from the thermal analysis described in Section D.

It is of interest to note that during cooldown the material temperature will lag the coolant temperature and, therefore, the steady state pressure, which is evaluated at the coolant temperature, will initially yield the lower maximum allowable pressure. When the thermal gradients increase, the stresses do likewise, and, finally, the transient analysis governs the maximum allowable pressure. Hence a point-by-point

comparison must be made between the maximum allowable pressures produced by steady state analyses and transient thermal analysis to determine the minimum of the maximum allowable pressures.

### 3. Core Operation

At all times that the reactor core is critical, the temperature must be higher than that required for inservice hydrostatic testing, and in addition, the pressure-temperature relationship shall provide at least a 40°F margin over that required for heatup and cooldown operations. Thus the pressure-temperature limit curves for core operation may be constructed directly from the inservice leak and hydrostatic test and heatup analysis results.

#### D. Thermal Stress Analysis

The equivalent linear stress due to thermal gradients is obtained from a detailed thermal analysis of the vessel. The temperature distribution in the vessel wall is governed by the partial differential equation

$$\rho c T_t - K \left[ (1/r) T_r + T_{rr} \right] = 0 \quad (15)$$

subject to initial condition

$$T(r, 0) = T_0, \quad (16)$$

and boundary conditions

$$-K T_r(r_i, t) = h \left[ T_c(t) - T(r_i, t) \right], \quad (17)$$

and

$$T_r(r_0, t) = 0 \quad (18)$$

where

$$T_c = T_0 + Rt. \quad (19)$$

$\rho$  is the material density,  $c$  the material specific heat,  $K$  the heat conductivity of the material,  $h$  the heat transfer coefficient between the water coolant and vessel material,  $R$  the heating rate,  $T_0$  the initial coolant temperature,  $T(r, t)$  the temperature distribution in the vessel,  $r$  the spatial coordinate, and  $t$  the temporal coordinate.

A finite difference solution procedure is employed to solve for the radial temperature distribution at various time steps along the heatup or cooldown cycle. The finite difference equations for  $N$  radial points, at distance  $\Delta r$  apart, across the vessel are:

for  $1 < n < N$

$$\begin{aligned} T_n^{t+\Delta t} = & \left[ 1 - \frac{\Delta t K}{\rho c (\Delta r)^2} \left( 2 + \frac{\Delta r}{r_n} \right) \right] T_n^t \\ & + \frac{\Delta t K}{\rho c (\Delta r)^2} \left[ \left( 1 + \frac{\Delta r}{r_n} \right) T_{n+1}^t + T_{n-1}^t \right], \end{aligned} \quad (20)$$

for  $n = 1$

$$\begin{aligned} T_1^{t+\Delta t} = & \left[ 1 - \frac{\Delta t K}{\rho c (\Delta r)^2} \left( 1 + \frac{\Delta r}{r_1} \right) - \frac{\Delta t h}{\rho c (\Delta r)} \right] T_1^t \\ & + \frac{\Delta t K}{\rho c (\Delta r)^2} \left[ \left( 1 + \frac{\Delta r}{r_1} \right) T_2^t + \frac{\Delta r h}{K} T_c^t \right], \end{aligned} \quad (21)$$

and for  $n = N$

$$T_N^{t+\Delta t} = \left[ 1 - \frac{\Delta t K}{\rho c (\Delta r)^2} \right] T_N^t + \frac{K \Delta t}{\rho c (\Delta r)^2} T_{N-1}^t \quad (22)$$

For stability in the finite difference operation, we must choose  $\Delta t$  for a given  $\Delta r$  such that both

$$\frac{\Delta t K}{\rho c (\Delta r)^2} \left( 2 + \frac{\Delta r}{r_1} \right) \leq 1 \quad (23)$$

and

$$\frac{\Delta t K}{\rho c (\Delta r)^2} \left( 1 + \frac{\Delta r}{r_1} \right) + \frac{\Delta t h}{\rho c (\Delta r)} \leq 1 \quad (24)$$

are satisfied. These conditions assure us that heat will not flow in the direction of increasing temperature, which, of course, would violate the second law of thermodynamics.

Since a large variation in coolant temperature is considered, the dependence of  $(K/\rho c)$ ,  $K$ , and  $h$  on temperature is included in the analysis by treating these as constants only during every  $5^\circ\text{F}$  increment in coolant temperature and then updating their values for the next  $5^\circ\text{F}$  increment. The dependence of  $(K/\rho c)$  called the thermal diffusivity and  $K$ , the thermal conductivity, can be determined from the ASME Boiler and Pressure Vessel Code, Section III, Appendix I - Stress Tables. A linear regression analysis of the tabular values resulted in the following expressions:

$$K(T) = 38.211 - 0.01673 * T \text{ (BTU/HR-FT-}^\circ\text{F)} \quad (25)$$

and

$$k(T) = (K/\rho c) = 0.6942 - 0.000432 * T \text{ (FT}^2\text{/HR)} \quad (26)$$

where T is in degrees Fahrenheit.

The heat transfer coefficient is calculated based on forced convection under turbulent flow conditions. The variables involved are the mean velocity of the fluid coolant, the equivalent (hydraulic) diameter of the coolant channel, and the density, heat capacity, viscosity, and thermal conductivity of the coolant. For water coolant, allowance for the variations in physical properties with temperature may be made by writing\*

$$h(T) = 170 (1 + 10^{-2} * T - 10^{-5} * T^2) v^{0.8} / D^{0.2} \quad (27)$$

where v is in ft/sec, D in inches, the temperature is in °F, and h is in Btu/hr-ft<sup>2</sup>-°F. The values for the heat-transfer coefficient given by this relationship are in good agreement with those obtained from the Dittus-Boelter equation for temperatures up to 600°F. The mean velocity of the coolant, v, is generally given in terms of the effective coolant flow rate Q (Lbm/hr) and effective flow area A (ft<sup>2</sup>). Given the relationship

$$\rho(T) = 62.93 - 0.48 \times 10^{-2} * T - 0.46 \times 10^{-4} * T^2 \quad (28)$$

for the density of water as a function of temperature, the mean velocity of the coolant is obtained from

$$v = Q / (3600 * \rho(T) * A) \quad (29)$$

---

\* Glasstone, S., Principles of Nuclear Reactor Engineering, D. Van Nostrand Co., Inc., New Jersey, pp. 667-668, 1960.

The thermal stress distribution is calculated from

$$\sigma_T(r, t) = \frac{\alpha E}{1-\nu} \left[ \frac{1}{r^2} \int_{r_i}^r T(r, t) r dr - T(r, t) + \frac{1}{r^2} \left( \frac{r_o^2 + r_i^2}{r_o^2 - r_i^2} \right) \int_{r_i}^{r_o} T(r, t) r dr \right] \quad (30)$$

where  $\alpha$  is the coefficient of thermal expansion (in/in °F),  $E$  is Young's modulus, and  $\nu$  is Poisson's ratio. This expression can be obtained from Theory of Elasticity by Timoshenko and Goodier, pp. 408-409, when imposing a zero radial stress condition at the cylinder inner and outer radius. Poisson's ratio is taken to be constant at a value of 0.3 while  $\alpha$  and  $E$  are evaluated as a function of the average temperature across the vessel

$$T_{avg} = \frac{2}{(r_o^2 - r_i^2)} \int_{r_i}^{r_o} T(r) r dr \quad (31)$$

The dependence of the coefficient of thermal expansion on temperature is taken to be

$$\alpha(T) = 5.76 \times 10^{-6} + 4.4 \times 10^{-9} * T \quad (32)$$

and the dependence of Young's modulus on temperature is taken to be

$$E(T) = 27.9142 + 2.5782 \times 10^{-4} * T - 6.5723 \times 10^{-6} * T^2 \quad (33)$$

as obtained from regression analysis of tabular values given in Section III, Appendix I of the ASME Boiler and Pressure Vessel Code.

The resulting stress distribution given by Equation (30) is not linear; however, an equivalent linear stress distribution is determined from the resulting moment. The moment produced by the nonlinear



stress distribution is given by

$$M(t) = b \int_{r_i}^{r_o} \sigma_T(r, t) r dr \quad (34)$$

where  $b$  is a unit depth of the vessel. Here we note that the moment is a function of time, i. e., coolant temperature via  $T_c = T_o + Rt$ . For a linear stress distribution we have that

$$\sigma_{\max} = \frac{Mc}{I} \quad (35)$$

where  $\sigma_{\max}$  is the maximum outer fiber stress,  $c$  the distance from the neutral axis, taken to be  $(r_o - r_i)/2$ , and  $I$  the section area moment of inertia which is given by

$$I = \frac{bh^3}{12} = \frac{b(r_o - r_i)^3}{12} \quad (36)$$

Combining these expressions results in the equivalent linear stress due to thermal gradients

$$\sigma_{\max} = \sigma_{bt} = \frac{6}{(r_o - r_i)^2} \int_{r_i}^{r_o} \sigma_T(r, t) r dr \quad (37)$$

The thermal stress intensity factor  $K_{It}$  is then defined as

$$K_{It} = M_b \sigma_{bt} \quad (38)$$

where  $M_b$  is determined from the curves given in Figure 1 wherein  $M_b = 2/3 M_m$ . It is of interest to note that a sign change occurs in the stress calculations during a cooldown analysis since the thermal gradients

produce compressive stresses at the vessel outer radius. This sign change must then be reflected in the  $K_{It}$  calculation for the cooldown analysis.

Normalized temperature and thermal stress distributions during a typical reactor heatup are given in Figure 4. The radial temperature is shown normalized with respect to the average temperature,  $T_{avg}$ , by

$$T = \frac{T - T_{avg}}{(T - T_{avg})_{max}} \quad (39)$$

The thermal stress and equivalent linearized stress, as calculated by Equations (30) and (37), are normalized with respect to the maximum thermal stress. Here we note that the actual thermal stress at the  $3/4T$  location is considerably less than the maximum equivalent linear stress which yields additional safety margins during the heatup cycle. Similar temperature and thermal stress distributions are developed during cooldown. The trends are nearly identical as those shown in Figure 4 when the inner and outer vessel locations are reversed with the  $1/4T$  location becoming the critical point.

#### E. Example Calculations

The following example is based on a reactor vessel with the following characteristics:

Inner Radius	=	82.00 in.	( $r_i$ )
Outer Radius	=	90.00 in.	( $r_o$ )
Operating Pressure	=	2250 psig	( $P_o$ )

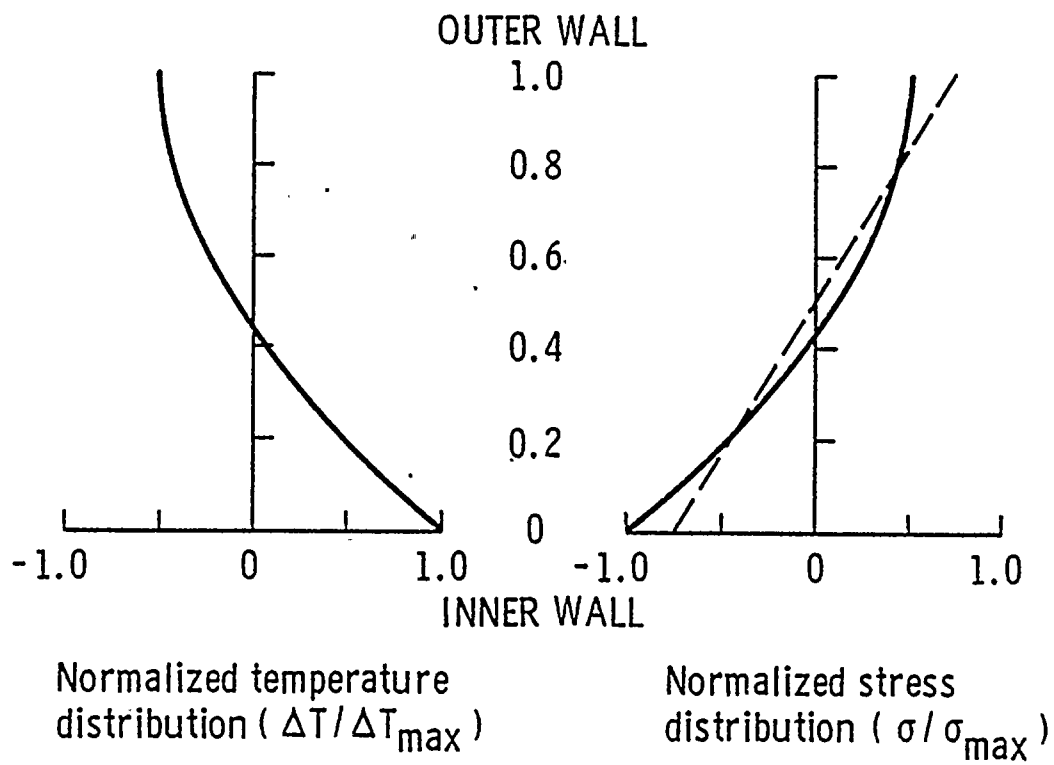


Figure 4. Typical Normalized Temperature and Stress Distribution During Heatup

Initial Temperature	=	70°F	(T <sub>o</sub> )
Final Temperature	=	550°F	(T <sub>f</sub> )
Effective Coolant Flow Rate	=	100 x 10 <sup>6</sup> Lbm/hr	(Q)
Effective Flow Area	=	20.00 ft <sup>2</sup>	(A)
Effective Hydraulic Diameter	=	10.00 in.	(D)
RT <sub>NDT</sub> (1/4T)	=	200°F	
RT <sub>NDT</sub> (3/4T)	=	140°F	

In the thermal stress analysis 21 radial points were used in the finite difference scheme. Going from 70°F to the final temperature of 550°F, approximately 12,000 time (temperature via  $T = T_o + Rt$ ) steps were required in the thermal analysis for the 100°F/hr heatup rate. The results of the computation are shown in Figures 5 through 9.

Figure 5 gives the reference stress intensity factor,  $K_{IR}$ , as a function of temperature indexed to RT<sub>NDT</sub> (1/4T). For the steady state analysis,  $K_{IR}$  is converted directly to allowable pressure via Equation 12.

During the heatup and cooldown thermal analyses the material temperature at the 1/4T and 3/4T and thermal stress intensity factors  $K_{It}$  are required to compute allowable pressure via Equations (13) and (14). The material temperatures versus coolant temperature during the 100°F/hr heatup and cooldown analyses are given in Figure 6. These temperatures allow computation of the corresponding reference stress intensity factors,  $K_{IR}$  (3/4T) and  $K_{IR}$  (1/4T). Figure 7 gives the corresponding thermal stress intensity factor at the 3/4T and 1/4T locations as a function of coolant temperature.

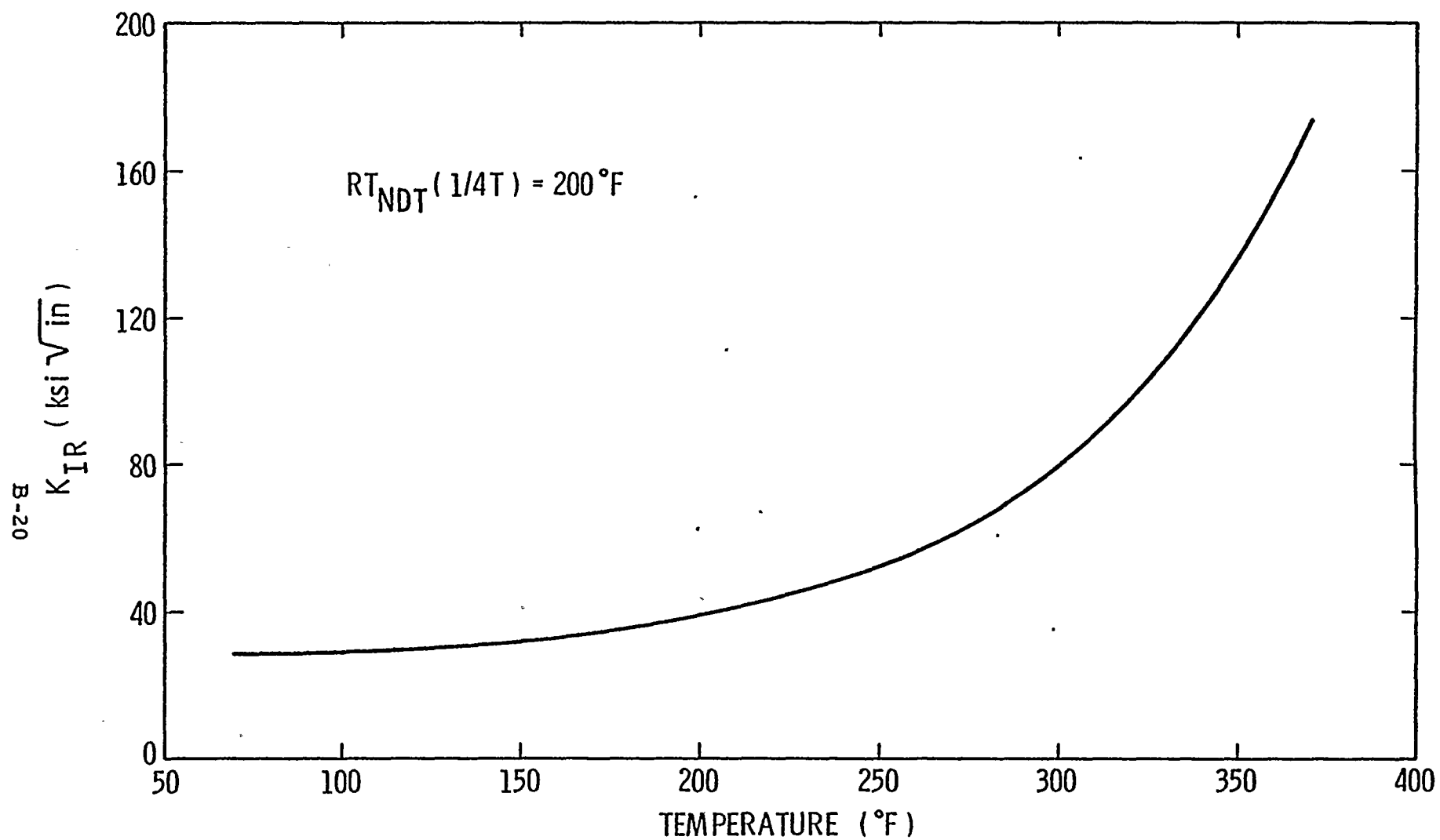


Figure 5. Reference Stress Intensity Factor as a Function of Temperature Indexed to  $RT_{NDT} (1/4T)$

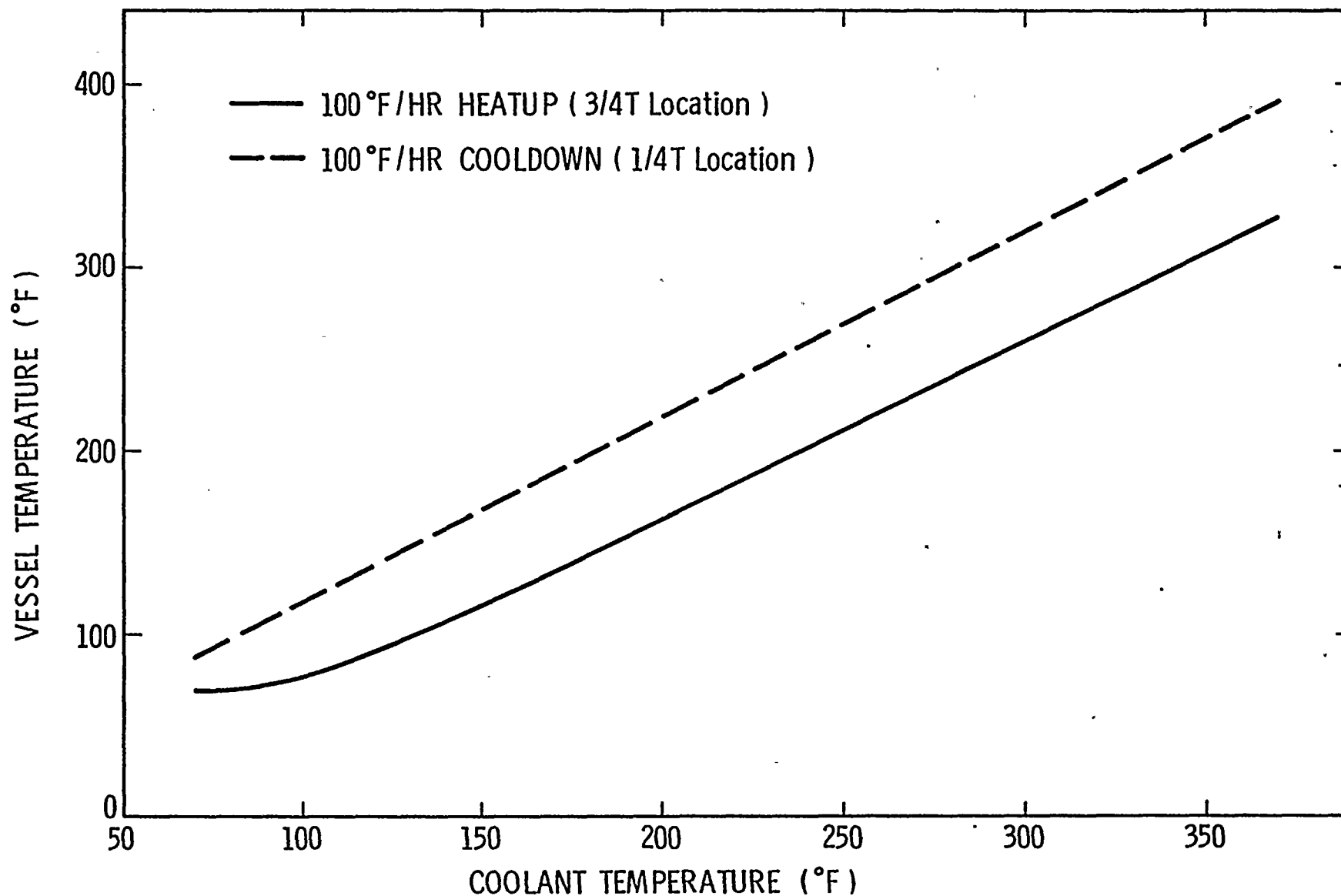


Figure 6. Vessel Temperature at 1/4T and 3/4T Locations as a Function of Coolant Temperature

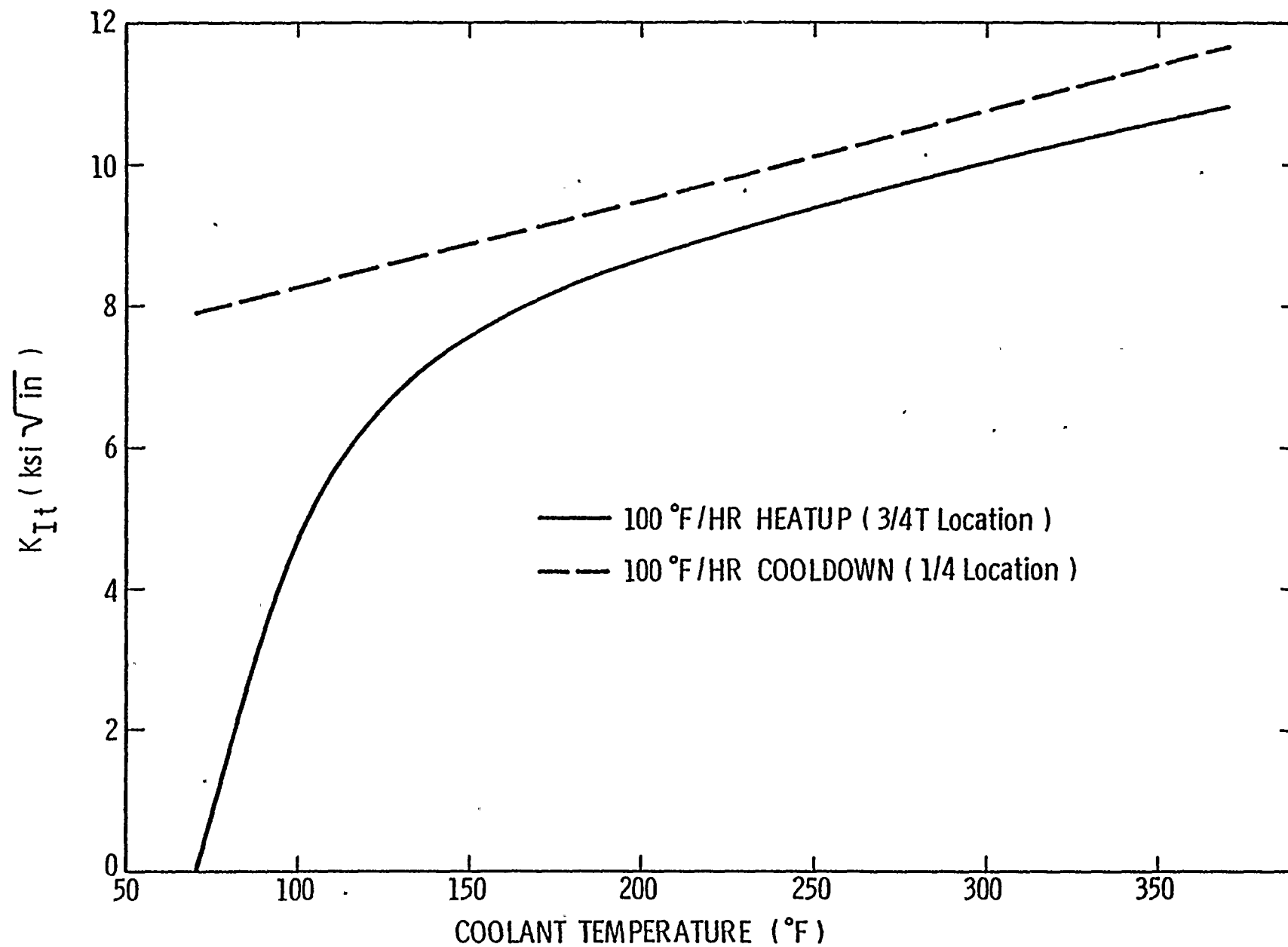


Figure 7. Thermal Stress Intensity Factor at 3/4T and 1/4T Locations as a Function of Coolant Temperature

Figures 8 and 9 demonstrate the construction of the allowable composite pressure and temperature curves for the 100°F/hr heatup and cool-down rates. The composite curves represent the lower bound of the thermal and steady state curves with the addition of margins of +10°F and -60 psig for possible instrumentation error. Figure 8 also shows the leak test limit, corrected for instrument error, as obtained from Equation (9). The limit points are at the operating pressure 2250 psig and at 2475 psig which corresponds to 1.1 times the operating pressure. The criticality limit is also shown in Figure 8 and is constructed by providing for a 40°F margin over that required for heatup and cooldown and by requiring that the minimum temperature be greater than that required by the leak test limit.



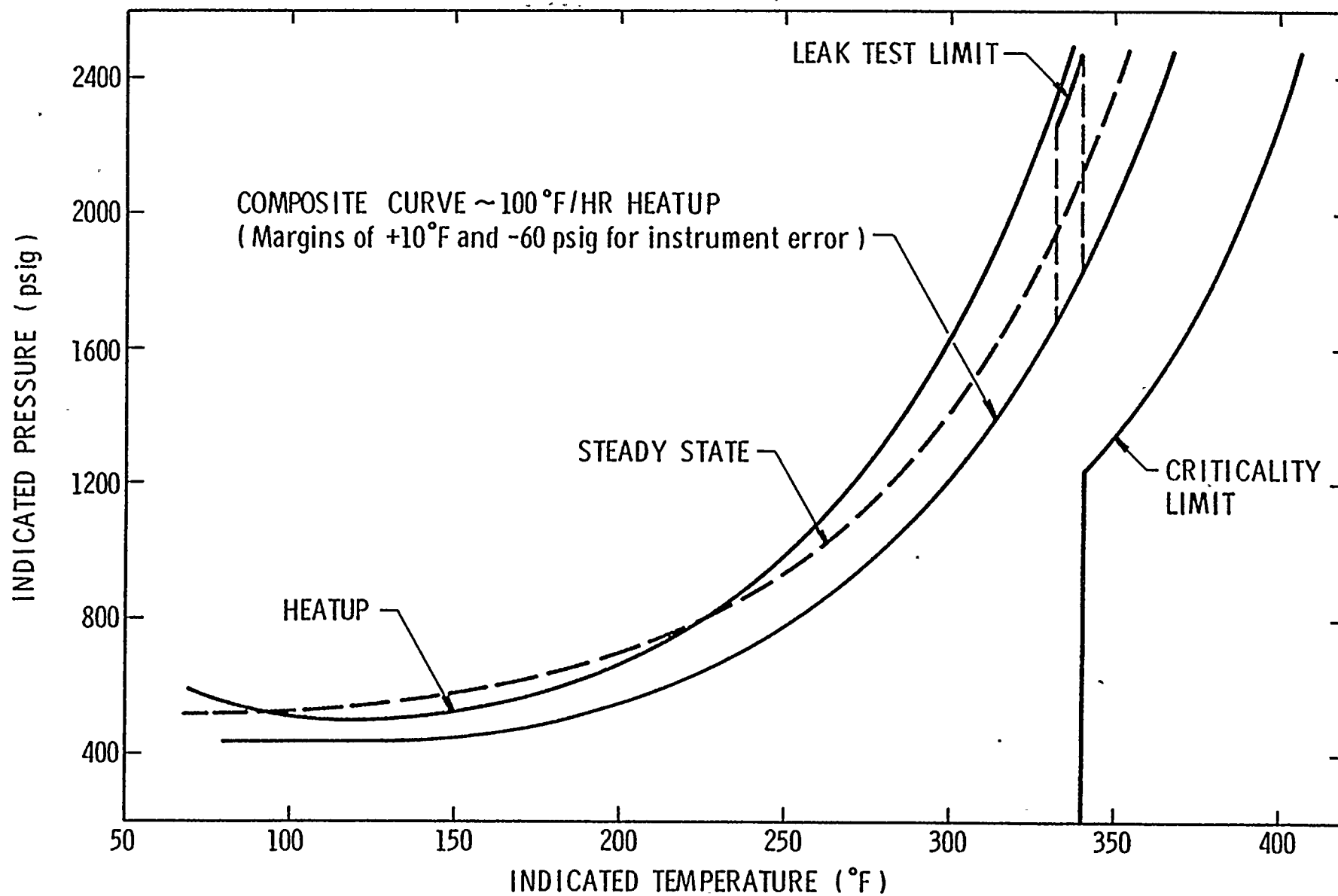


Figure 8. Pressure-Temperature Curves for 100°F/Hr Heatup

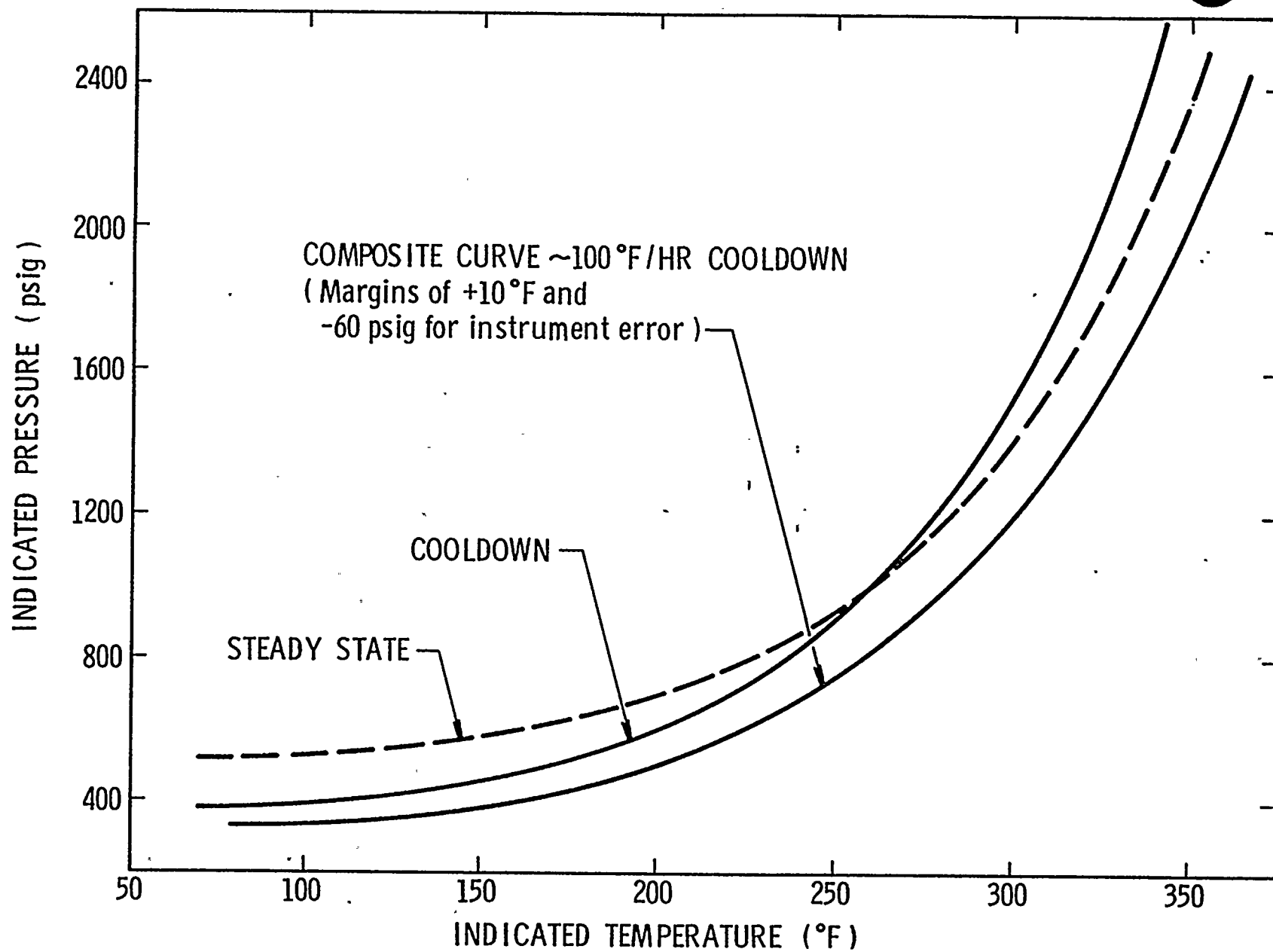


Figure 9. Pressure-Temperature Curves for  $100^{\circ}\text{F}/\text{Hr}$  Cooldown



ADDENDUM TO FINAL REPORT  
ON  
"REACTOR VESSEL MATERIAL SURVEILLANCE PROGRAM FOR  
DONALD C. CGOK UNIT NO. 1, ANALYSIS OF CAPSULE T"

<u>30 ft-lb C<sub>v</sub> Temp. (deg F)</u>	<u>Plate B4406-3</u>		<u>Weld</u>	<u>Weld</u>	<u>Correlation</u>
	<u>(Long.)</u>	<u>(Trans.)</u>	<u>Metal</u>	<u>HAZ</u>	
Irradiated	65	90	-10	20	105
Unirradiated	.5	20	-90	-100	45
ΔT	60	70	80	120	60

<u>Monitor</u>	<u>Weight</u>
<u>Identification</u>	<u>(mg)</u>
Fe - Top	18.2
Fe - Top Mid.	15.3
Fe - Mid.	17.2
Fe - Bot. Mid.	16.6
Fe - Bot.	16.4
Cu - Top Mid.	64.9
Cu - Mid.	62.9
Cu - Bot. Mid.	70.9
Ni - Top Mid.	22.9
Ni - Mid.	25.5
Ni - Bot. Mid.	24.5
Co - Top	9.3
Co(Cd) - Top	8.7
Co - Bot.	9.5
Co(Cd) - Bot.	7.7
U-238	12.0(a)
NP-237	20.0(a)

(a) As reported in WCAP-8047.

ADDENDUM NO. 2 TO FINAL REPORT  
ON  
"REACTOR VESSEL MATERIAL SURVEILLANCE PROGRAM FOR  
DONALD C. COOK UNIT NO. 1, ANALYSIS OF CAPSULE T"

Additional Tensile Test Data

<u>Specimen No.</u>	<u>Fracture Load (psi)</u>	<u>Fracture Stress (psi)</u>	<u>Uniform Elongation<sup>(a)</sup> (%)</u>
A1	64,700	188,600	5.00
A2	63,250	177,000	2.45
W9	87,600	250,000	4.56
W10	75,800	193,700	2.87

---

(a) Using method of change in cross-sectional area of unnecked portion of specimen per ASTM E 184-62.